Mesoporous silica nanoparticles as protein carriers for antibiofilm applications

Master's thesis by

Kia Peura

Pharmaceutical Sciences
Faculty of Science and Engineering
Åbo Akademi University
Åbo, Finland
2021

ACKNOWLEDGEMENTS

First and foremost, I would like to express my special thanks to my laboratory supervisor, Anna Slita, who guided me throughout this project by planning the protocols and teaching me how to operate different analysis machines and how to analyze the data. Research for her Phd thesis gave me the opportunity to do this project with the topic of Mesoporous silica nanocarriers as protein carriers for antibiofilm applications.

Also, I want to present my special thanks to Prakirth Govardhanam, who taught me in practice how to synthetize and analyze MSNs and how to study drug release.

I want to thank my supervisor Jessica Rosenholm for her advice and comments on the written thesis. Also, I want to present my gratitude to Tapani Viitala, who gave me valuable comments and feedback to this thesis.

At last, but not least, I would like to thank my partner, Guillem Saldo Rubio, for his support. He was there to help me and give me motivation throughout working on this project.

ABSTRACT

Multidrug resistant (MDR) bacteria are currently one of the biggest public health threats. About 60 to 70% of bacterial infections are associated with formation of biofilms that are a cause of a wide variety of chronic infections. Biofilms are bacterial communities embedded within an extracellular polymeric substance matrix (EPS) which consists of lipids, polysaccharides, proteins, and nucleic acids. Biofilms protect bacteria effectively from external threats, such as antibacterial agents. Current antimicrobial research aims to affect the structure of the biofilm and, in this way, enhance the effects of antibacterial agents.

In this thesis, large pore (10 nm) mesoporous silica nanoparticles (MSNs) were examined as potential antibacterial protein carriers for antibiofilm applications. A loading protocol for proteins with similar sizes to the used model protein, bovine serum albumin (BSA), resulted in an average loading capacity of 30%. Biofilm formation and the changes in biofilm growth was studied to validate that MSNs do not have intrinsic antimicrobial effects. Short-term *in vitro* protein release studies conducted in pHs corresponding to the pH gradient within biofilms unveiled premature release of protein cargo.

This project demonstrated that MSNs can be a potential drug delivery system (DDS) for therapeutic proteins and could be exploited for antibiofilm applications. The use of nanosized drug delivery systems (DDSs) could improve penetration and accumulation of antibiotics in biofilms and provide enhanced efficacy and reduced side-effects of antimicrobial therapeutics.

Keywords: Nanoparticle, Mesoporous silica nanoparticles, Biofilm, Drug delivery system

Table of Contents

1 List of abbreviations

APTES = (3-aminopropyl) triethoxysilane

BSA = bovine serum albumin

CTAC = cetyltrimethylammonium chloride

DDS = drug delivery systems

DLS = dynamic light scattering

DMSO = dimethyl sulfoxide

DSC = differential scanning calometry

EPS = extracellular polymeric substance

FITC = fluorescein isothiocyanate isomer I

HEPES = 4-(2-hydroxyethyl)-1-piperazineethanesulfonic acid

HPLC = high performance liquid chromatography

LC% = loading capacity

LB = Luria Bertani

MDR = multidrug resistant

MES = 2-(*N*-morpholino) ethanesulfonic acid

MSNs = mesoporous silica nanoparticles

MWCO = molecular weight cut-off

NPs = nanoparticles

PBS = phosphate-buffered saline

PdI = polydispersity index

PEG = polyethylene glycol

PEI = polyethyleneimine

pI = isoelectric point

GRAS = generally recognized as safe

SiNPs = silica nanoparticles

SPR = surface plasmon resonance

TEA = triethanolamine

TEM = transmission electron microscopy

TEOS = tetraethyl orthosilicate

TRITC = tetramethylrhodamine

2 Introduction

Multidrug resistant (MDR) bacteria are currently one of the biggest public health threats. Approximately 700,000 patients have died from MDR bacterial infections globally each year (Song et al., 2021). It has been estimated that by the year 2050, MDR bacteria will be causing over 10 million deaths a year. About 60 to 70% of bacterial infections are associated with the formation of biofilms which causes a wide variety of chronic infections (Xiu et al., 2020). Bacterial biofilms protect bacteria effectively with several mechanisms that help to cope with environmental stress and allow microbes in biofilms to display an antibiotic resistance up to 1000 times higher than their planktonic counterparts (Ceri et al., 1999). Additionally, biofilms accelerate the spread of resistance genes by offering a favorable milieu for horizontal transfer of genetic material (Angles et al., 1993; Hausner & Wuertz, 1999). Currently, there are only a few effective antibiotics left to treat infections caused by MDR bacteria, and their effectiveness is reduced significantly when these bacteria form biofilms (Song et al., 2021).

To combat MDR bacteria, novel approaches in antibiotic research are needed. Currently, no drug products have been approved to specifically treat biofilm-related infections (Song et al., 2021). One of the main challenges is the delivery of antibiotics to bacterial biofilms so that therapeutic concentrations of the drug are achieved. Nanomedicine provides novel tools to combat this issue; nanosized carriers have been examined as drug delivery systems (DDS) of antimicrobials into biofilms (Xiu et al., 2020). The advantages of nanosized DDS include improved penetration and accumulation of antibiotics in biofilms, providing enhanced efficacy and reduced side-effects. The research of novel DDS needs to be developed in tandem with novel antimicrobial therapeutics to overcome the problem of MDR bacteria.

In this thesis, mesoporous silica nanoparticles (MSNs) were studied as potential antibacterial protein carriers for antibiofilm applications. MSNs were chosen due to their tuneability, low price and good biocompatibility. The use of therapeutically active proteins was not in the scope of this study; therefore, a place holder protein (i.e., bovine serum albumin, BSA) was used to set a baseline for the protein loading protocol and analysis of the loaded MSNs.

2.1 Bacterial biofilms

Naturally occurring bacteria can be found as planktonic (free flowing) or sessile (attached) cells. The sessile stages, bacterial biofilms, are present both on inert and living surfaces, such as on chronic wounds and medical devices (Flemming et al., 2016). All known microorganisms form biofilms, which are highly organized microbial communities exhibiting activities that can be compared to bustling cities. Usually, one biofilm consists of several different species of bacteria and other microorganisms, including fungi, protozoa, algae, and viruses (Muhammad et al., 2020). A biofilm is, thus, the dominant microbial lifestyle. Studies have shown that bacterial biofilms form in multiple steps, require intercellular signaling to function, and have a different gene transcription from planktonic bacteria (Watnick & Kolter, 1999; Davies et al., 1998; Prigent-Combaret et al., 1999)

In bacterial biofilms, microorganisms are enclosed in a self-produced viscous matrix known as the extracellular polymeric substance (EPS) (Flemming et al., 2000). EPS is a hydrogel that consists of water and cellular materials, such as lipids, proteins, polysaccharides, and nucleic acids. EPS forms most of the bacterial biofilm, and its composition varies between different environments and bacterial species. Biofilms are usually highly heterogenous; they can contain several microenvironments with different pH gradients, signaling chemicals and oxygen concentrations (Lewandowski, 2000). Hidalgo et al. (2009) reported a pH gradient of 5 to 7 within an *E. coli* biofilm, and Fulaz et al. (2019) reported similar results within a *P. fluorescens* biofilm. Schlafer et al. (2018) have reported pH gradients as low as 4 in the center of microcolonies of several different bacterial species. To maximize survival, bacteria can either alter gene expression or distribute themselves according to who can survive best in each environment (Watnick & Kolter, 2000). This ability to adapt and self-organize is especially important within multispecies biofilms. The principal purpose of a biofilm is to provide protection and accumulate nutrition for bacteria and other microorganisms living in it. EPS provides the crucial properties of biofilms, as it offers structural stability and protection from environmental threats such as antimicrobials and phagocytes (Flemming et al., 2000). The properties of the antibacterial tolerance of biofilms will be further discussed in 2.1.1.

The formation of a bacterial biofilm is a multistep process in which intercellular signaling is required (Davies et al., 1998) (**Figure 1**). Biofilm formation starts with planktonic bacteria slowly approaching a surface and forming reversibly associations with the surface or other microbes attached to the surface (Watnick & Kolter, 1999). After an interaction with a suitable substrate, bacteria bind irreversibly and multiplication into microcolonies can start. These microcolonies commence to produce EPS which then embeds all the surrounding bacteria. After enough successful replications, these microcolonies have formed tower- or mushroom-like structures. When the biofilm has grown to a size which is no longer beneficial for the bacterial survival, focal areas of the biofilm are released to spread and form new biofilms. Abandoning the biofilm is a significant part for the survival of the community. To leave the biofilm, bacteria produce a specific chemical, polysaccharide lyase, which enables their final detachment from the biofilm (Watnick & Kolter, 2000). Bacteria have been shown to undergo morphological changes to adapt to the changes in their environment; planktonic bacteria present flagella, tail-like structures constructed of protein filaments, that allow them to actively seek more favorable environments and move through a liquid medium, while sessile bacteria lack such a feature (Garrett et al., 1999).

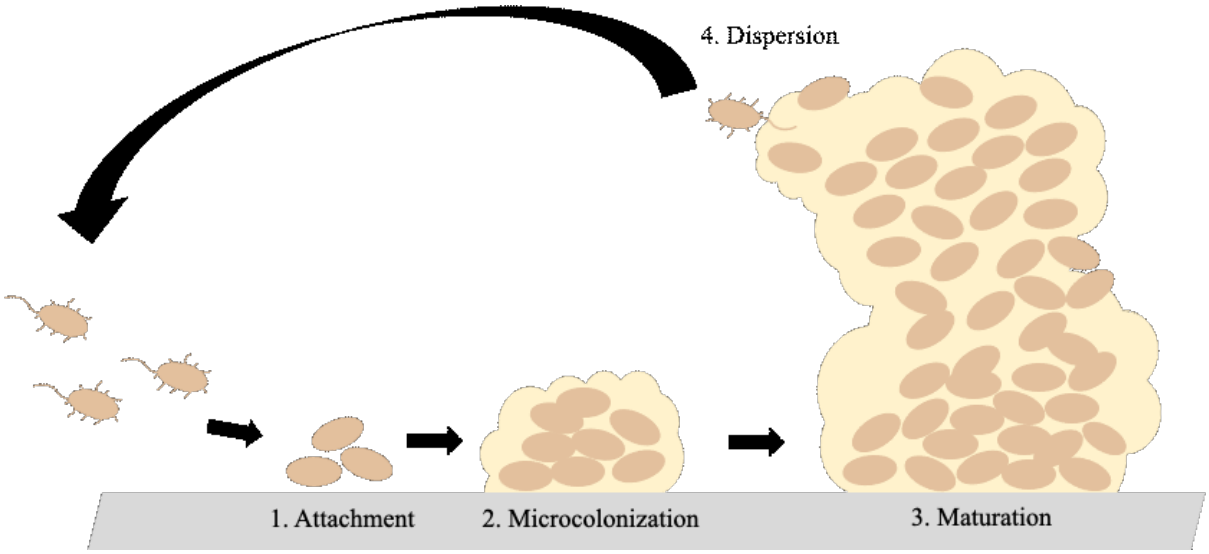

Figure 1 The life cycle of biofilms. The formation of biofilms can be divided into four distinct steps; 1. Attachment, where planktonic bacteria form interactions with the surface, 2. Microcolonization, where bacteria multiply and commence to produce extracellular polymetric substance (EPS), 3. Maturation, where the biofilm grows to its final size and performs the usual actions of a biofilm, and 4. Dispersion, which the biofilm reaches when it has grown to a size no longer beneficial, and bacteria are released from the biofilm to seek more favorable environments to be able to start a new biofilm formation.

Bacterial communication within a biofilm is called quorum sensing; it is intercellular signaling which enables bacteria to communicate with each other in groups and enables coordinated responses to the environment (Davies et al., 1998). Quorum sensing regulates gene expression within the bacterial community depending on signals received from neighboring bacteria; bacteria produce specific signaling molecules, autoinducers, which increase in concentration as a function of cell density (McLean et al., 1997). Autoinducers can diffuse from one cell and enter another cell allowing bacteria to communicate both within and between different species. Detection of these signaling molecules causes a stimulation that alters gene expression of the receiver cell, which can lead to a variety of physiological activities, such as antibiotic production or biofilm formation. Several different classes of autoinducers have been identified, such as acylated homoserine lactones (acyl-HLs) primarily produced by Gram-negative bacteria (e.g., *Escherichia coli*), oligopeptides predominantly produced by Gram-positive bacteria (e.g., *Staphylococcus aureus*) and furanosyl borate diester, which is known to be produced by bioluminescent marine bacteria (e.g., *Vibrio harveyi*) (McLean et al., 1997**;** Fuqua et al., 1998; Dong et al., 2005). Quorum sensing is highly beneficial for bacteria, as the ability to communicate and share information allows bacteria to form highly organized structures and aids bacteria to defend themselves more effectively (Waters & Bassler, 2005). It also contributes to the ability of the bacteria to infect host organisms, making them more pathogenic by enforcing the gene expression of virulence factors.

Bacteria are more likely to acquire new genetic material within a biofilm than in the form of planktonic cells. Studies suggest that gene transfer, especially through conjugation, occurs within biofilms with enhanced efficiency (Hausner et al., 1999). Conjugation is a bacterial gene transfer mechanism in which one bacterium transfers genetic material to another through direct contact. This type of transfer of genetic material may occur rapidly in biofilms where bacteria are closely associated with each other. Biofilms, thus, serve as a perfect milieu for microevolution and for bacteria to share antibiotic resistance genes, virulence factors and other properties enhancing bacterial survival.

2.1.1 Biofilms as part of antibacterial resistance

Pathogenic bacteria are known to produce biofilms, which protects them from antibacterial therapeutics by physically limiting their penetration, regulating multidrug efflux, and

enhancing resistance genes among their bacterial members (Mah & O'Toole, 2001). Bacteria within a biofilm have been shown to have 10 to 1000 times more resistance to antibiotics than planktonic cells (Ceri et al., 1999). Consequently, biofilms are highly difficult to eradicate. Biofilms cause chronic and recurrent infections everywhere in the body; biofilm-related infections include for example chronic wounds, endocarditis (infection in the heart), recurrent sinusitis (nasal infection) and otitis (middle ear infection) (Hall-Stoodley & Stoodley, 2009). Biofilms form also on medical implants and on contact lenses, causing a continuous risk of severe infections.

Multiple factors contribute to the resistance of biofilms. Bacteria within a biofilm have been shown to present reduced metabolic activity caused by reduced nutrient availability, and reduced growth rates, which have been linked to reduced effectiveness of antibiotics that target rapidly multiplying cells (Mah et al., 2001). EPS protects the bacterial community from various external threats, such as antibacterial agents and phagocytes, by physically limiting their penetration into the biofilm. Surface attachment reduces the net negative charge of bacterial cells and enhances the stability of the biofilm membrane (John et al., 2011). Biofilms also demonstrate specific resistance mechanisms due to the altered physiology of biofilm bacteria compared with planktonic bacteria (Mah et al., 2001).

Multidrug efflux pumps are highly abundant in bacterial biofilms (Blanco et al., 2016). These pumps are transporters that extrude toxins, such as antibiotics and heavy metals, from the biofilm to protect bacteria. Prokaryotes present five major families of efflux transporters, which differ in substrate specificity, membrane location and energy source. Enzymatic modifications of antibiotic targets are another factor enhancing antibiotic resistance within bacterial biofilms (Schaenzer & Wright, 2020). Also, integral structure-functions of the biofilm offer effective innate tolerance (Mah et al., 2001). Biofilm associated bacteria are more resistant to toxic substances such as antibiotics, chlorine, and detergents. Biofilm-specific substances such as exopolysaccharide and the quorum sensing specific effects part-take the resistance properties.

2.1.2 Therapeutic approaches in antibiofilm applications

Although biofilms were first discovered already in the 1650s by a Dutch microbiologist, Antonie van Leeuwenhoek, bacteria have almost exclusively been studied as single species

planktonic cultures (Hoiby, 2017). It was not until in the late 20th century that scientific interest in biofilms grew and understanding of the biofilm nature increased. However, even though several studies have demonstrated that bacteria grow rather as communities than as single cells, antibiotic research has mostly focused on planktonic bacteria. Biofilms have been shown to have high tolerance for antimicrobial properties of the immune system, antiseptics, and antibiotics (Mah et al., 2001). Therefore, it is crucial to concentrate on how to eradicate biofilms instead of how to kill a single planktonic bacterium.

Several different approaches are under current research to find an effective technique to eradicate biofilms. Attempting to reduce the adhesion of bacterial biofilms is one of the currently studied approaches. Reducing the adhesion of bacterial biofilms can be obtained by using polymers that alter the surface (Beloin et al., 2014). Materials combining ester and cyclic hydrocarbon moieties have been shown to display anti-adhesive activity *in vitro* in *E. coli, P. aeruginosa* and *S. aureus* (Hook et al., 2012). Another antibiofilm approach is targeting biofilm maturation (Beloin et al., 2014). This can be done by blocking the maturation process through inhibition of signaling pathways, such as quorum sensing. Reducing persisters formation is a novel approach that has raised scientific interest and it is expected to reveal new therapeutic strategies. Persisters are bacterial cells within the biofilm, that have entered a specific phenotype state which allows them to survive in the presence of 1000-fold the minimum inhibitory concentration of antibiotics.

It has been studied that some microorganisms outcompete other species by producing antibiofilm agents, which can inhibit biofilm development, disturb cell-to-cell communication and/or enhance the dispersal of target biofilms (Fang et al., 2018). Fang et al. showed in their study in 2018 that probiotic *E. coli* could inhibit the biofilm formation of pathogenic *E. coli* as well as the biofilm formation of *S. aureus* and S. *epidermis*. They were able to link a protein called DegP as a significant factor for this inhibiting action. DegP is a periplasmic protein that has chaperon functions at low temperature and proteolytic activities at higher temperatures. This protein has been strongly linked to the virulence of several pathogens, as the lack of DegP has been proved to increase the vulnerability of bacteria. It is likely that DegP modifies or binds to the target cell structure in some unknown manner, which then results in biofilm inhibition.

One of the most relevant challenges in the treatment of chronic infections is the effective delivery of antibiotics into bacterial biofilms. The use of nanoparticles (NPs) as a delivery vehicle for antimicrobials is a strategy that could potentially combat the setbacks of antimicrobial resistance (Xiu et al., 2020). By using NPs as carriers, the mode of uptake by the pathogens can be tailored and, thus, issues associated with antimicrobial resistance mechanisms such as hyperactive efflux pumps can be avoided. NPs can also be used for optimal drug loading and targeted delivery of antimicrobials, which reduces the regularly used high doses and toxic side effects.

2.2 Mesoporous silica nanoparticles (MSNs)

Nanotechnology and engineered nanomaterials have been increasingly studied for novel applications both in industry and in the medical field of research. Nanotechnology is a branch of science studying materials and their properties on the nanoscale (1 nm - 1000 nm). Nanotechnology in the medical field of research, known as nanomedicine, has shown significant benefits for developing more precise and effective therapeutics as well as novel tools for diagnosis and bioimaging (Min et al., 2015). Nanomedicine provides opportunities to tackle problems such as low local drug concentrations, poor intracellular drug penetration, and limited crossing of biological barriers. The use of nanosized drug carriers has been widely studied for specific targeting and more effective intracellular delivery of drug molecules (Torchilin, 2012).

For drug delivery applications, silica nanoparticles (SiNPs) engineered from amorphous silica have been widely exploited due to their beneficial characteristics such as large surface area, wide design flexibility, and good biocompatibility (Selvarajan et al., 2020). Silica (silicon dioxide, SiO_2) is a natural substance found in all living organisms and in the environment, as one of the most abundant minerals, quartz (Iler, 1979). Silica has been classified as generally recognized as safe (GRAS) by the United States Food and Drug Administration (FDA) and is widely used in many applications, such as an additive in food (E551) and as an excipient in pharmaceuticals (Diab et al., 2017; FDA, 2022). Silica is easily degraded via hydrolysis forming orthosilicic acid and silicate oligomers in water media (Bindini et al., 2020). In literature, variants of SiNPs have been explored as an effective tool

for targeted delivery of therapeutic molecules, allowing enhanced efficacy, higher drug-loading amounts, and faster release (Tang et al., 2012).

SiNPs can be synthetized with several different structures; they can be solid, hollow, chrysanthemum-like, spherical, rodlike, or mesoporous. Mesoporous silica nanoparticles (MSNs) present a structure with uniform pores with a size from 2 nm to 50 nm, providing an increased surface area and usually dendrite-like porous structure (Shen et al., 2014). All characteristics of MSNs, such as the rigid silica framework, nanochannels/pores, and the outer surface, can be distinctly modified. Porous SiNPs are especially suitable to be used as nanocarriers; the pore structure can be used as a container for therapeutic drug molecules and the silica framework as a protective shell. The outer surface can be easily modified for the purpose of targeted drug delivery and to ensure cell uptake of the whole nanocarrier system (Tang et al., 2012).

2.2.1 MSNs as nanocarriers for therapeutic proteins

Today, macromolecular therapeutics comprise an increasing share of novel drug molecules entering the market (Bhutani et al., 2021). Protein therapeutics are favored to combat a wide variety of diseases due to their remarkable specificity *in vivo* compared to small molecular therapeutics. However, the intracellular delivery of therapeutic proteins is causing continuous challenges due to their large size (typically 3-6 nm in diameter) and poor stability (Milo & Phillips, 2015). Nanoparticle-based drug delivery has shown potential to tackle these problems and MSNs are of special interest as potential protein carriers due to their stable structure and tunable surface chemistry with well-defined pore structure and easily controllable morphology (Tang et al., 2012).

Drug delivery applications using porous SiNPs have previously been limited to small molecular therapeutics (molecular size <2 nm), due to challenges in synthetizing uniform monodispersed MSNs with uniform large pore sizes (>5 nm) suitable for *in vivo* applications. Only during the past decade researchers discovered appropriate synthesis methods for large pore MSNs. By now, MSNs have been examined to enhance stability, activity, responsive release, and intracellular delivery of proteins (Deodhar et al., 2017; Liu & Xu, 2019). Results show that proteins can be loaded into these porous nanocarriers. Moreover, the absorption

process of the protein to these nanocarriers can be tuned with changes in surface chemistry and choice of reaction solvent. As a result, proteins can be confined within the pores, allowing the silica framework to protect the macromolecules from environmental threats, such as enzymes and changes in pH, which increases the stability and lengthens the half-life of the macromolecules.

2.2.2 MSN synthesis and modifications

SiNPs can be synthetized by several protocols with a size range of 10-500 nm and with different shapes and physicochemical properties (Selvarajan et al., 2020). The most common synthesis methods for SiNPs include the Stöber method and the microemulsion method. The Stöber method yields non-porous SiNPs with sizes less than 200 nm (Stöber et al., 1968). In the microemulsion method, the size of the NP yield is dependent on the volume of the used nanoreactors. A modified Stöber method has been used to synthetize MSNs with a wide range of different pore sizes (Selvarajan et al., 2020). In 2014, Shen and his colleagues presented a method, known as the biphase stratification approach, which provides a robust and easy way to synthetize uniform monodispersed mesoporous nanoparticles with a ‘‘dendritic’’ pore structure with large and tunable pore sizes applicable for protein delivery (Shen et al., 2014).

2.2.2.1 Biphase stratification reaction system

According to the above-mentioned synthesis protocol reported by Shen et al., MSNs can be synthetized in a heterogenous oil-water biphase stratification reaction system, where the synthesis reaction occurs at the interface. The oil phase in this method is a tetraethyl orthosilicate (TEOS) solution and the aqueous phase contains cationic cetyltrimethylammonium chloride (CTAC) as a template and the organic base triethanolamine (TEA) as a catalyst. The particles are created in a two-generation process within a single reaction flask, wherein the first generation creates a seed and a core of the MSNs upon which the second generation creates the dendritic mesochannel funnels (**Figure 2**). (Shen et al., 2014)

The synthesis reaction begins with a nucleation process at the interface of the oil and aqueous solution. Silica from the TEOS reservoir slowly leaks towards the aqueous phase, where it hydrolyses and forms an oligomer that orients itself on the hydrophobicity gradient of the interface. This leak towards the aqueous phase provides a high enough concentration at the interphase for nucleation to happen. The formed oligomers can go into the aqueous phase to trigger the nucleation process when the critical nucleation concentration has been reached. Stirring of the reaction flask allows the formed nanoseeds to contact the interface, which allows oligomers from the interface to assemble on top of the growing seeds. This process can be repeated to achieve the desired core size of the particle. (Shen et al., 2014)

The second-generation synthesis takes place in the aqueous phase after the nanoseeds have grown too large to stay in the oil-water hemimicelles and can start the Y-type dendritic mesochannel growth. The nucleation concentration needed for this step is much lower than the critical nucleation concentration for the first generation, thus this process can take place fully in the aqueous phase. The final pore size can be tuned from 2.8 nm to 13 nm by changing the amount of the used organic solvent, such as cyclohexane. (Shen et al., 2014)

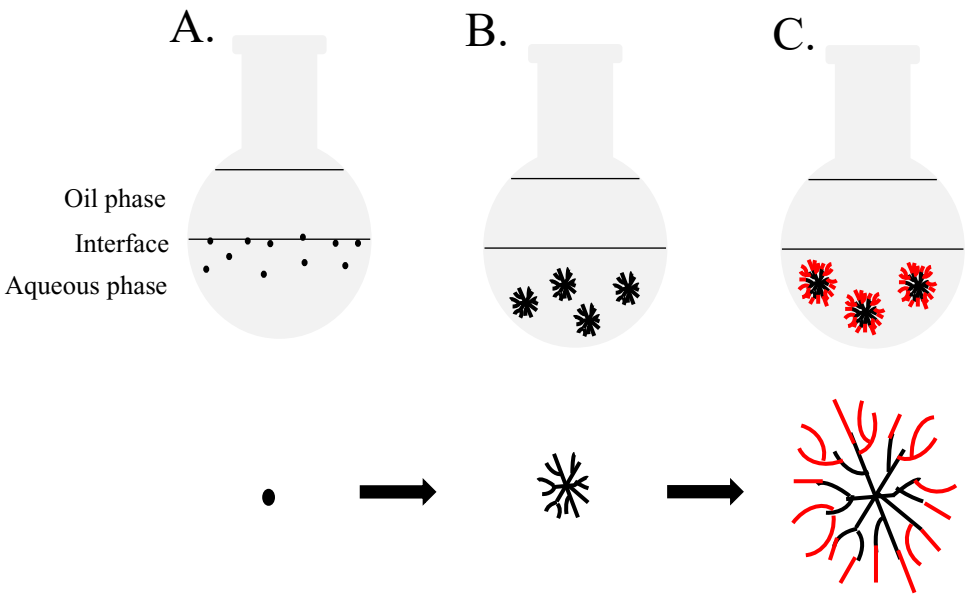

Figure 2 Synthesis process of mesoporous silica nanoparticles (MSNs) in an oil-water biphase stratification system in a two-generation process. The synthesis reaction occurs in the oil-water interface, where the oil phase contains tetraethyl orthosilicate (TEOS), which acts as the silica reservoir, and the aqueous phase containing cetyltrimethylammonium chloride (CTAC) acting as a template for the reaction. In the first-generation process, (A.) formation of nanoseeds takes place at the interface, after which (B.) the formed nanoseeds can go to the aqueous solution to trigger the nucleation process. During the second-generation synthesis (C.) the dendritic mesochannel growth occurs fully in the aqueous solution.

2.2.2.2 Surface modifications

The ease of functionalization is one of the many perks of MSNs. The surface of MSNs consists of a high content of silanol groups (Si-OH) providing a favorable site for covalent modifications (Selvarajan et al., 2020). Different surface probes can be attached either via co-condensation, which entails the modified functional groups also inside the pores, or post-synthetic grafting, which principally conjugates the functional groups on the surface. Surface modification can be employed to improve colloidal stability as well as biocompatibility of the MSNs (D'souza & Shegokar, 2016; Selvarajan et al., 2020). Attachment of polyethylene glycol (PEG) is often used to improve colloidal stability, but it also provides a stealth mode of action allowing the NPs to circulate longer in the blood stream and functions as a gatekeeper for cargos loaded in the pores (Jokerst et al., 2011; Cui et al., 2012). Fluorescent probes, peptides, and drugs can also be conjugated covalently on the MSN surface (Selvarajan et al., 2020).

Polyethyleneimine (PEI) grafting has been used for controlled drug delivery (Wang et al., 2018). PEI grafting is performed with the use of aziridine, also known as ethyleneimine, which is a highly reactive monomeric organic compound that undergoes polymerization when treated with acids and forms polymeric derivatives, polyethyleneimines (Sweeney, 2002) and can readily be used to grow from surfaces from e.g., -OH groups present on MSNs (Rosenholm et al., 2006). PEI grafting changes the naturally negative surface charge of the SiNPs to positive, which can be employed to enhance drug loading of negatively charged therapeutics by electrostatic attraction.

2.2.3 Biocompatibility of MSNs

Biocompatibility and biodegradability are major elements when choosing materials for medical applications. For nanomaterials, properties such as particle size, shape, surface area, and structure all play a role in the biocompatibility of the particles. SiNPs have a GRAS classification from FDA and are naturally degraded by hydrolysis, however, toxicity studies have demonstrated size-dependent compatibility with larger particle sizes triggering acute systemic toxicity (Zhao et al., 2011; Leclerc et al., 2012). Tuning of physicochemical

parameters, such as surface charge or particle size, can affect the biocompatibility of SiNPs and, thus, the physicochemical characteristics should be carefully managed to ensure safety.

Surface modifications can significantly affect the biocompatibility of SiNPs. Cationic surface charge has been shown to increase the cytotoxicity and immune response of NPs, while bare silanol groups on the SiNP surface might interact unfavorable with biological molecules and negative net surface charge causes an accelerated clearance by macrophages (Tang et al., 2012). PEGylation provides a stealth effect; it can hide the NPs from immune system resulting in reduced toxicity and increased blood-circulation time. Similarly, lipid coatings have been shown to improve biocompatibility and prolonged the half-lives of SiNPs.

As part of evaluation of the safety profile, elimination and degradation processes of the particles should be investigated carefully. According to previous studies, degradation products of SiNPs are eliminated either through feces or urine depending on the particle size and charge (Selvarajan et al., 2020). Principally larger particles and positively charged particles are excreted through gastrointestinal tract, while smaller particles (< 6 nm) are excreted rapidly via urinary tract.

3 Aims

This thesis project aims to investigate the benefits of MSN-based carriers for protein delivery and examine the use of MSN-protein complexes in antibiofilm applications. The specific goals of the project are as follows:

- To synthetize and modify MSNs so that they can be used as protein carriers.
- To successfully load a model protein into modified MSNs.
- To investigate the effects of the MSN-protein complex on bacterial biofilms.
- To investigate short-term *in vitro* protein release from the MSNs.

The hypothesis is that MSNs can be used as protein nanocarriers and that they can be exploited to help proteins to enter biofilms and protect them from degradation. It is expected

that the protein can be released from the carrier within the pH gradient of a bacterial biofilm. The MSNs are not expected to show enhanced antibacterial action without an antibiofilm actor when in contact with cell cultures.

4 Materials and methods

4.1 Synthesis and characterization of MSNs

The MSNs synthesis was carried out according to the biphase stratification system protocol presented in 2.2.2. The pore size was adjusted to 10 nm by controlling the hydrophobic solvents and the concentration of silica source in the upper oil phase. Non-labelled (optically transparent) MSNs were synthetized for general protein loading and characteristics studies, while labelled (fluorescent) MSNs were synthetized to enable imaging. All synthetized MSNs were modified with PEI grafting to change the net surface charge of the NPs from negative to positive to optimize protein loading.

4.1.1 Synthesis of MSNs

The synthesis solution was prepared with 36 ml of deionized water (Milli-Q, Turku), 24 ml of 25 wt.% of CTAC in H_2O (Sigma Aldrich) and 160 µl of >99.0% TEA (Sigma Aldrich) and was incubated for an hour in a 60 °C paraffin oil bath. 20 ml of 10% v/v TEOS solution was prepared from 98% TEOS (Sigma Aldrich) in 99.5% cyclohexane (Sigma Aldrich) and added to the synthesis solution which was then incubated overnight in a 60 °C paraffin oil bath. The formed oil phase was removed, and the synthesis solution was centrifuged at 37,700 x g for 10 minutes at 18 °C. The supernatant was discarded. To remove the residues of the synthesis solutions, the particles were washed with ethanol (Etax Aa) and centrifuged at 37,700 x g for 10 minutes at 18 °C. The waste ethanol was removed. The particles were redispersed in 30 ml of 0.6 w% ammonium nitrate (NH_4NO_3) in ethanol (Etax Aa) extraction solution and incubated for six hours in a 60 °C paraffin oil bath. The solution was centrifuged at 37,700 x g for 10 minutes at 18 °C. The supernatant was discarded, and the particles were left at room temperature overnight. The extraction steps were repeated to ensure that all

residues were removed. To remove the extraction solution, the particles were washed with ethanol (Etax Aa) and centrifuged at 37,700 x g for 10 minutes at 18 °C. The supernatants were discarded. The MSN stock solution was prepared by adding 10 ml of ethanol (Etax Aa) and stored at 4 °C.

4.1.2 Synthesis of fluorescent MSNs

8.6 mg/ml FITC-conjugation solution of >90% fluorescein isothiocyanate isomer I (FITC) (Sigma Aldrich) in ethanol (Etax Aa) was prepared into a small HPLC (high performance liquid chromatography) cuvette and sonicated until completely dissolved. The HPLC cuvette was placed on a magnetic stirrer and put under vacuum for 10 minutes. While under vacuum, 15 µl of 99% (3-aminopropyl) triethoxysilane (APTES) (Sigma Aldrich) was added, and the reaction was let to occur for two hours under vacuum.

The synthesis solution was prepared with 36 ml of deionized water (Milli-Q, Turku), 24 ml of 25 wt.% of CTAC in H_2O (Sigma Aldrich) and 160 µl of >99.0% TEA (Sigma Aldrich) and incubated for an hour in a 60 °C paraffin oil bath. 1 ml of a FITC-conjugation solution and 20 ml of a 10% v/v TEOS solution of 98% TEOS (Sigma Aldrich) in 99.5% cyclohexane (Sigma Aldrich) were added to the synthesis solution which was then incubated overnight in a 60 °C paraffin oil bath. The formed oil phase was removed, and the synthesis solution was centrifuged at 37,700 x g for 10 minutes at 18 °C. The supernatant was discarded. To remove the residues of the synthesis solutions, the particles were washed with ethanol (Etax Aa) and centrifuged at 37,700 x g for 10 minutes at 18 °C. The waste ethanol was removed. The particles were redispersed in 30 ml of 0.6 w% ammonium nitrate (NH_4NO_3) in ethanol (Etax Aa) extraction solution and incubated for six hours in a 60 °C paraffin oil bath. The solution was centrifuged at 37,700 x g for 10 minutes at 18 °C. The supernatant was discarded, and the particles were left at room temperature overnight. The extraction steps were repeated to ensure that all residues were removed. To remove the extraction solution, the particles were washed with ethanol (Etax Aa) and centrifuged at 37,700 x g for 10 minutes at 18 °C. The supernatants were discarded. The FITC-labelled MSN stock solution was prepared by adding 10 ml of ethanol (Etax Aa) and stored at 4 °C.

4.1.3 PEI grafting

First, 100 mg of MSNs was redispersed in 10 ml of anhydrous 99.8% Toluene (Sigma Aldrich). Ethanol (Etax Aa) was added to increase the volume to allow centrifugation. The sample was centrifuged at 37,700 x g for 10 minutes at 18 °C. Supernatant was discarded and the sample was redispersed in 10 ml of toluene, after which it was transferred to a 100 ml flask. Another 10 ml of toluene was added, and the flask was placed in a paraffin oil bath at 60 °C. 5.2 µl of 100% acetic acid and 52 µl of aziridine was added to the solution, which was then incubated in the paraffin oil bath at 60 °C overnight. Aziridine, also known as ethyleneimine, is a highly reactive monomeric organic compound that undergoes polymerization when treated with acids and forms polymeric derivatives, polyethyleneimines (PEIs) (Sweeney, 2002).

On the following day, 10 ml of toluene was added to the sample, which was then centrifuged at 32,700 x g for 15 minutes at 18 °C. The supernatant was discarded. The sample was washed twice with ethanol (Etax Aa) by centrifuging the sample redispersed in ethanol at 32,700 x g for 10 minutes at 18 °C. Stock solution of PEI-grafted MSNs was prepared in ethanol (Etax Aa) and stored at 4°C.

4.1.4 Characterization of MSNs

Determination of the hydrodynamic particle size (⌀ nm) and surface charge was done with dynamic light scattering (DLS) and ζ-potential techniques with Zetasizer nanoseries (Malvern instruments). The hydrodynamic size, Z-average and polydispersity index (PdI) were measured, and the average value of triplicates was recorded. Samples for DLS measurements were 1% dilution of the investigated particle suspension in deionized water (Milli-Q, Turku) and measured in a HPLC cuvette. Samples for ζ-potential measurements were 10% dilution of the investigated particle suspension in 4-(2-hydroxyethyl)-1-piperazineethanesulfonic acid (HEPES) buffer and measured in a folded capillary cuvette.

Concentrations of the prepared MSN stock solutions were investigated by adding 500 µl of the stock solutions into a 1 ml Eppendorf, whose weight was known. The samples were then centrifuged twice at 9,000 x g for 10 minutes, to separate the NPs from the liquid media.

The samples where dried overnight in a vacuum, and the weight of the NPs was measured the following day.

Transmittance electron microscopy (TEM) image was taken of one batch of the MSNs to visualize and confirm the size and uniformity of the NPs. The average size and standard deviation of four MSNs visualized in TEM image was reported as a comparison for the hydrodynamic particle size determined with DLS analysis.

4.2 Labelling of bovine serum albumin (BSA)

First, 20 ml of 2 mg/ml BSA solution was made by dissolving BSA (Sigma Aldrich) in 0.1 M sodium carbonate solution (Na_2CO_3 in distilled water) (pH 9). The protein solution was combined at 4 °C with 1 ml of 1 mg/ml fluorescent tetramethylrhodamine (TRITC) conjugation solution of TRITC in dimethyl sulfoxide (DMSO). The light sensitive TRITC-BSA solution was prepared and let to react protected from light at 4 °C overnight.

TRITC-BSA solution was dialyzed using a dialysis bag of 3500 MWCO (molecular weight cut-off) against water for two days at room temperature. The water was changed each day. The TRITC-BSA solution was then freeze-dried by freezing the solution with liquid nitrogen for 5 minutes and then drying the frozen solution in a vacuum overnight. The freeze-dried fluorescent BSA was stored at -7 °C.

4.3 Protein loading

4.3.1 Determination of optimal loading pH

To choose the optimal pH for loading media, the charge of the protein was examined in 10 mM 2-(N-morpholino) ethanesulfonic acid (MES) buffer with pH 4, 5 and 6. For each pH, samples with five different BSA concentrations (1 mg/ml, 3 mg/ml, 5 mg/ml, 10 mg/ml, and 15 mg/ml) were prepared in MES, and the pHs were adjusted as needed. The ζ-potential was measured for each sample with Zetasizer nanoseries (Malvern instruments).

4.3.2 Protocol for loading

Protein loading was performed for three different concentrations (1 mg/ml, 2 mg/ml, and 3 mg/ml) of either pure BSA (Sigma Aldrich) or labelled BSA to 3.0 mg of PEI-grafted (labelled or non-labelled) MSNs with a pore size of 10 nm. BSA stock solution of 10 mg/ml was prepared in 10 mM MES buffer (pH 4). For each sample, 3.0 mg of PEI-grafted MSNs was redispersed in 500 µl of 10 mM MES (pH 4) buffer with an ultrasonicator. Amounts corresponding to 1 mg, 2 mg or 3 mg were added to the samples from the BSA stock solution and MES was added to reach the total volume of 1 ml. The loading was performed by sonicating the samples for 30 seconds. The samples were centrifuged at 12,300 g for 20 minutes twice. The supernatants were collected after each centrifugation. The samples were redispersed in 1 ml of MES (pH 4). The samples with protein-loaded MSNs were freeze-dried by freezing the solution with liquid nitrogen for 5 minutes and then drying the frozen solution in a vacuum overnight. The samples were stored at -7 °C.

The amount of loaded protein was determined by measuring the BSA concentration of each supernatant with Nanodrop (NanoDrop 3300 Fluorospectrometer, Thermo scientific) at 280 nm, with control samples of 1 mg/ml, 2 mg/ml, and 3 mg/ml BSA in MES (pH 4). MES buffer (pH4) was used as blank. Loading capacity (LC%) was calculated regarding the total amount of protein measured in supernatants.

$$LC\% = \frac{(Total\ protein\ amount - Amount\ of\ protein\ in\ supernatants)}{Total\ nanoparticle\ weight} * 100\%$$

Particle size (⌀ nm), PdI and ζ-potential were measured for the loaded MSNs before freeze-drying with Zetasizer nanoseries (Malvern instruments). The ζ-potential of the samples was remeasured after freeze-drying. Samples for DLS measurements were made of 1% dilution of the investigated particle suspension in deionized water (Milli-Q, Turku) and measured in a HPLC cuvette. Samples for ζ-potential measurements were made of 10% dilution of the investigated particle suspension in HEPES and measured in a folded capillary cuvette.

4.3.3 Differential scanning calorimetry (DCS)

Differential scanning calorimetry (DSC) (DSC Q 2000, TA Instruments, US) heat-flow analysis were performed to PEI-grafted MSNs and to BSA-loaded PEI-grafted MSNs (with 1:3, 2:3, and 3:3 loading ratios) to identify and detect characteristic phase transitions. The samples (each with a weight between 3-6 mg) were measured against a reference sample. For the analysis 40 °C was used as the starting temperature, 10 °C as the heating rate and 200 °C as the highest temperature. The thermodynamic values were averaged with three measurements.

4.4 Biofilm analysis methods

4.4.1 Surface plasmon resonance (SPR)

A multi-parametric surface plasmon resonance (SPR) instrument (BioNavis) with four flow channels was used to study biofilm growth on a gold sensor and the effects of the MSNs and MSN-protein complex on the biofilm growth. A baseline was initially measured with LB (Luria Bertani) broth for 15 minutes with a flow rate of 7 ml/hour. Then, an *E. coli* suspension cultivated in LB was injected onto the gold sensor for 30 minutes with a flow rate of 7 ml/hour. The SPR measurement was then continued by running LB with a flow rate of 7 ml/hour to provide constant flow and nutrients for the forming biofilm.

In the first analysis performed, the growing of the biofilm was monitored for 21 hours followed by treating the formed biofilm with 20 ug/ml, 100 ug/ml, and 300 ug/ml of ampicillin, with no treatment as a control. The biofilm growth and the effect of the antibiotic on the biofilm growth were visualized in real-time sensorgrams produced by the SPR BioNavis instrument.

In the second analysis the biofilm was treated with MSNs (3 mg/ml), PEI-grafted MSNs (3 mg/ml) and BSA-loaded PEI-grafted MSNs (1:3 mg/ml) 1.5 hours after the bacteria was injected onto the gold sensor. The effect of the MSN samples on the biofilm growth was visualized in real-time sensorgrams produced by the SPR BioNavis instrument.

4.4.2 Confocal imaging

Initial *E. coli* bacterial culture was cultivated on an agar plate with LB at 37 °C overnight. 1:1000 dilution of the overnight culture was incubated at 37 °C for an hour. 3 ml of the 1:1000 dilution was spread on five separate agar plates. The plates were then placed on a shaker at 37 °C for 24 hours.

The cultivated bacterial cultures were treated for 48 hours with 1 ml of fluorescent BSA-loaded PEI-grafted MSN solution in LB and 500 µg/ml BSA solution in LB. Confocal images of the treated *E. coli* cultures were taken with an Evos microscope (Thermo Fisher) with green and red fluorescent filters. ImageJ software was used to create a composite image of the results.

4.5 Short-term *in vitro* protein release

Short-term protein release study of PEI-grafted MSNs loaded with BSA in phosphate-buffered saline (PBS) buffer was performed in three different pHs (6, 6.5, and 7) representing the pH gradient within *E. coli* biofilms (Hidalgo et al., 2009). For each pH, triplicates of seven time points (0 min, 30 min, 60 min, 90 min, 120 min, 180 min, and 240 min) with 0.5 mg/ml of BSA-loaded PEI-grafted MSNs were placed to a shaking water bath at 37 °C, and the absorbance was measured with a Lambda UV/visible spectrophotometer (UV-6300PC Double Beam Spectrophotometer, VWR international, China) at 285 nm at the corresponding time points. To confirm the total amount of BSA within the MSNs, leaching test was performed for 0.5 mg/ml BSA-loaded PEI-grafted MSNs in PBS by stirring the solution with a magnetic stirrer at room temperature for 30 minutes and the average BSA absorbance was measured in triplicates, with PBS (with pHs 6, 6.5 or 7) as a blank. The concentrations of released BSA were determined with standard curves corresponding to each pH and the average BSA concentration of the triplicates was presented as the result. Percentage of BSA released from the MSNs was plotted as a function of time with the total protein amount determined with leaching corresponding to 100%.

5 Results

5.1 MSN synthesis and characterization

The average hydrodynamic particle size (Ø nm), PdI and ζ-potential (mV) of MSNs, PEI-grafted MSNs, and fluorescent PEI-grafted MSNs are presented in **Table 1**. All measured NPs were within the size range of 145 to 200 nm. PEI grafting resulted in the desired change in the surface net charge from negative to positive. The characterization of the MSNs was done to ensure that the used method could reliably be used for the synthesis and that the yielded NPs were of the needed quality for further steps in this study.

Table 1 MSN characterization. Here, the characterization of optically transparent and fluorescent (FITC-conjugated) MSNs before and after PEI grafting is presented. Particle size (nm in diameter) is based on the average of Z-average values from DLS measurements, which calculate the average hydrodynamic size by the intensity of scattered light. PdI value presents the square of the standard deviation divided by the mean particle diameter. The ζ-potential value correlates to the net surface charge in millivolts (mV) in HEPES buffer measured at room temperature.

Sample	Particle size (Ø nm)	PdI	Zeta potential (mV)
MSNs	188 ± 5	0.14 ± 0.1	-18 ± 0.6
MSNs-PEI	177 ± 30	0.10 ± 0.1	+28 ± 3
FITC-MSNs	149 ± 4	0.23 ± 0.01	-6 ± 1
FITC-MSNs-PEI	185 ± 1	0.17 ± 0.1	+18 ± 1

A TEM image confirming the size and uniformity of MSNs is presented in **Figure 3**. It can be observed that the analyzed MSNs are monodispersed (containing particles of uniform size) and have the desired dendrite-like porous structure. The average size of four MSNs visualized in TEM presented an average diameter of 109 nm with a standard deviation of 1.7.

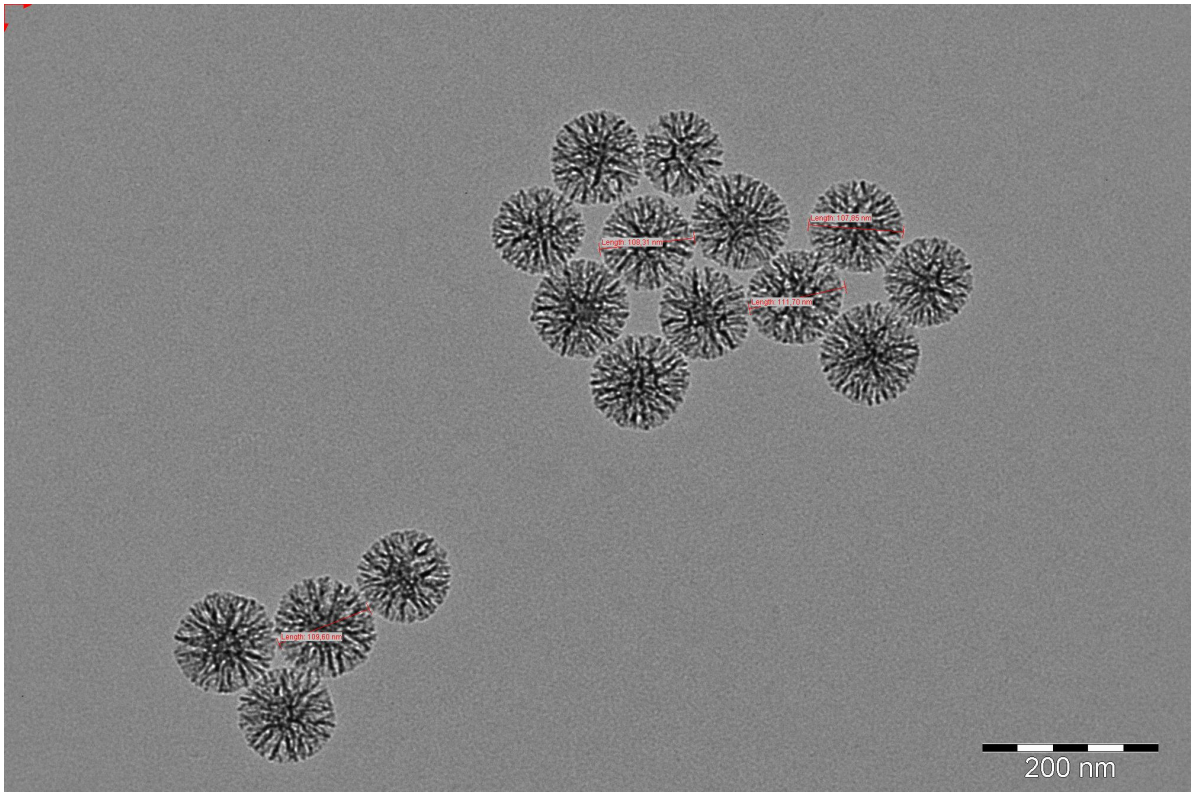

Figure 3 Transmission electron microscope (TEM) image of MSNs synthetized with biphase stratification protocol. The analyzed MSNs are of uniform size and with a radial symmetry. The average size of four of the observed MSNs visualized in the image is 109 nm, with a standard deviation of 1.7. Scale bar, 200 nm.

5.2 Protein loading and characterization of loaded MSNs

To create a suitable controlled environment for protein loading, the change in protein charge was studied in MES buffer at pH 4, 5, and 6. The results of the ζ-potential measurements of BSA in MES (pH 4, 5, and 6) are presented in **Figure 4**. At pH 6, BSA presented a negative net surface charge in all measured concentrations, while at pH 4 and 5, the net surface charge was close to neutral or slightly positive in 5 mg/ml to 1 mg/ml concentration range. At pH 4, BSA presented a negative net surface charge in concentrations 10 mg/ml and 15 mg/ml. Due to conformational information of BSA in different pHs from literature, MES buffer at pH 4 was chosen as the loading media for the loading protocol.

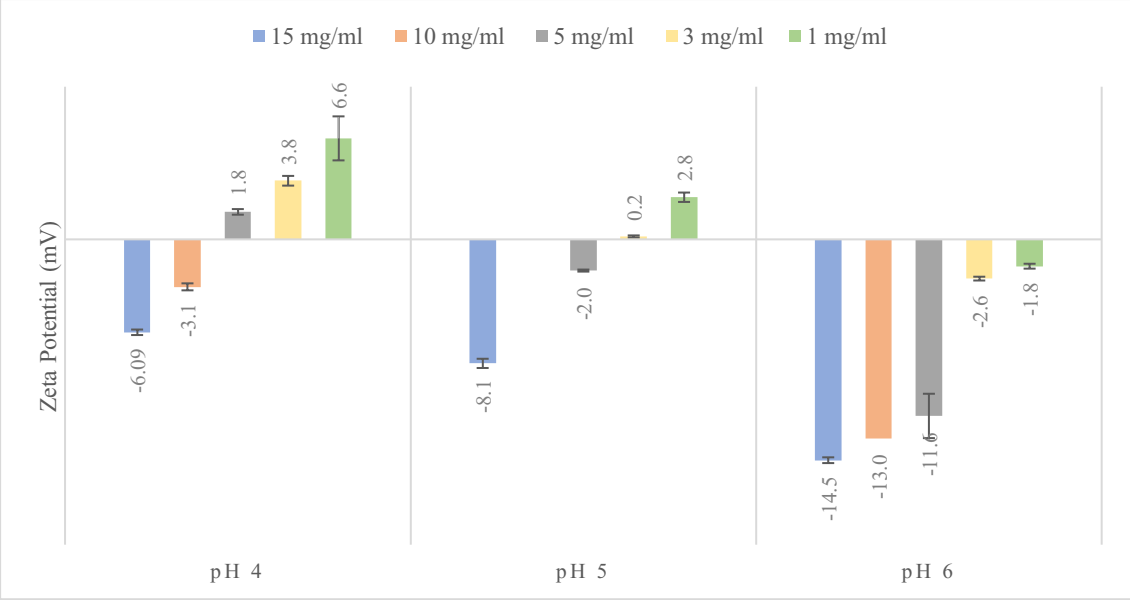

Figure 4 ζ-potential (mV) of BSA in MES (pH 4, 5, and 6). The change in surface charge of BSA was studied in three different pHs (4, 5, and 6) with four different concentrations (15 mg/ml, 10 mg/ml, 3 mg/ml, and 1 mg/ml). MES buffer with a pH of 4 was eventually chosen as the loading media for protein loading.

LC% was determined by BSA concentration measurements from the supernatants collected during loading. The BSA concentrations measured from supernatants are presented in **Figure 5**. The calculated LC% for each ratio used (1:3, 2:3, and 3:3 BSA to MSNs) are presented in **Table 2**. The average LC% of all measurements was 30%.

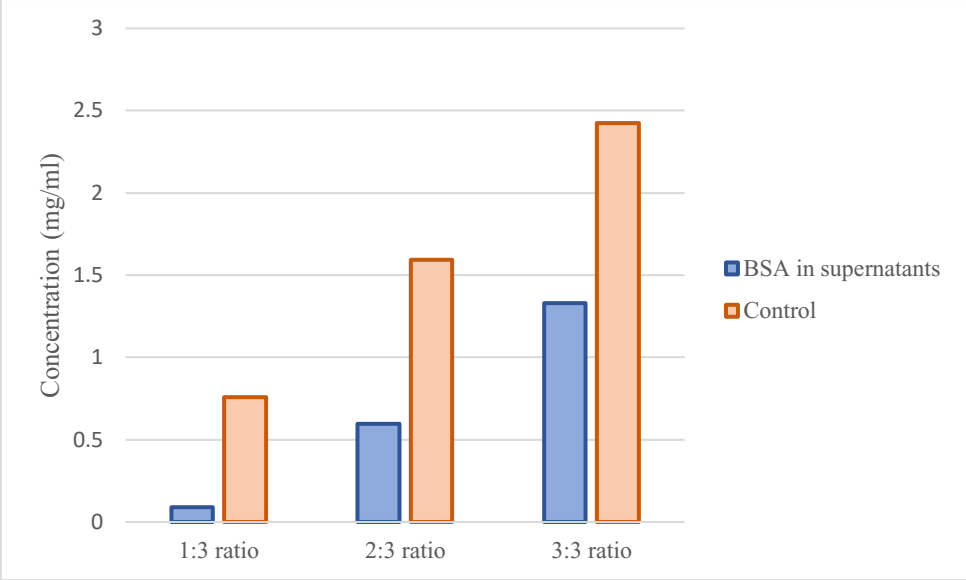

Figure 5 Total amounts of BSA residues after loading**.** The loaded PEI-grafted MSNs were washed twice, and the supernatants were collected for measuring the amount of BSA residues. Three loading ratios of BSA to MSNs were examined (1:3, 2:3, and 3:3) and the BSA residues were compared with control samples corresponding to total amount of BSA used in loading.

Table 2 Loading capacities (LC%) of BSA into PEI-grafted MSNs with a pore size of 10 nm. Loading was performed in three different ratios (1:3, 1:3, and 3:3) of BSA to MSN. The average LC% for all three ratios was 30%.

BSA to MSN (pore size 10 nm) ratio	Loading capacity (%)
1:3	22
2:3	33
3:3	36

The ζ-potential (net surface charge) of BSA-loaded PEI-grafted MSNs was measured before and after freeze-drying to investigate whether the used protocol affects the charge of the carrier system. In **Figure 6**, the average ζ-potential (mV) before and after freeze-drying of all used loading ratios of BSA to MSNs (1:3, 2:3, and 3:3) is presented. The change in surface charge of unloaded PEI-grafted MSNs in MES (pH 4) before and after freeze-drying is presented as a control. Freeze-drying resulted in an increase of positive net surface charge in all measured samples.

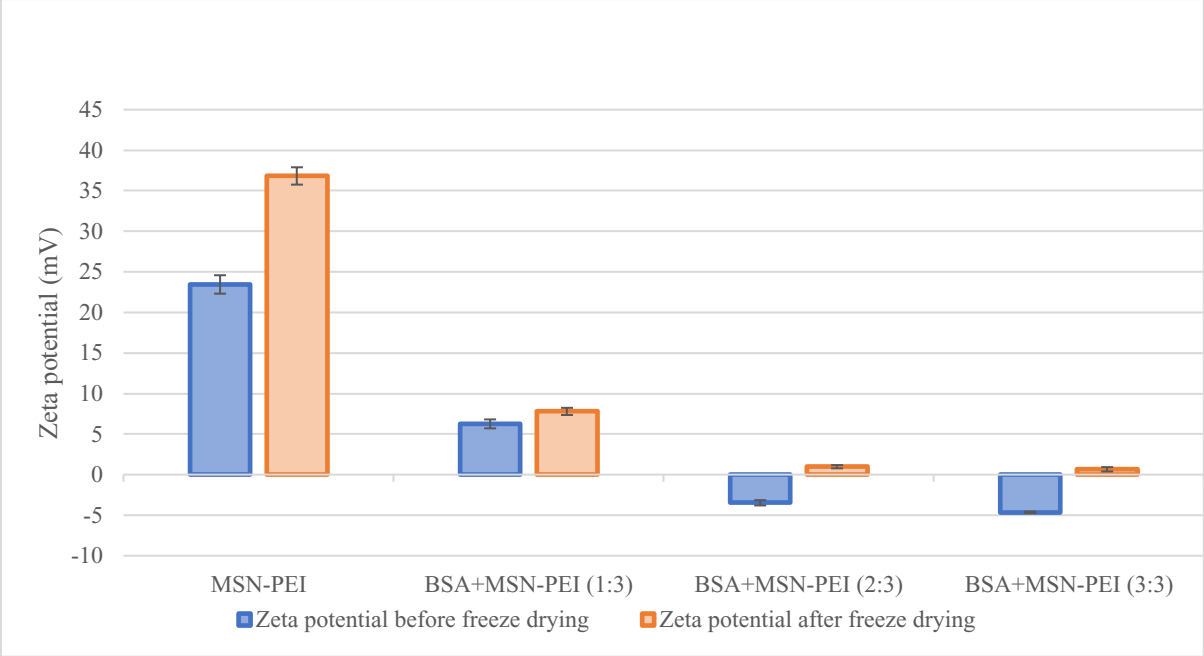

Figure 6 The effect of freeze-drying on ζ-potential. The change in surface charge was studied in each BSA concentration (1 mg/ml, 2 mg/ml, and 3 mg/ml) used for loading as well as in a control sample of unloaded PEI-coated MSNs.

DSC analysis was performed with pure BSA, unloaded PEI-grafted MSNs and to BSA-loaded PEI-grafted MSNs of three loading ratios (1:3, 2:3, and 3:3 BSA to MSNs) to compare the thermal changes, such as melting points, and to determine which part of the complex is responsible for which change. The results of the DSC heat flow analysis are presented in **Figure 7**. All samples containing BSA show a peak at 86 °C, while all samples containing PEI-grafted MSNs show a peak at 101 °C and at 166 °C. Pure BSA sample shows peaks also at 182 °C and 217 °C, while BSA-loaded PEI-grafted MSN samples show only a low slope between these temperatures. Significantly, the BSA and PEI-grafted MSN samples show distinct Heat Flow curves and the characteristics of each sample can be identified from the heat flow curves of samples of BSA-loaded PEI-grafted MSN

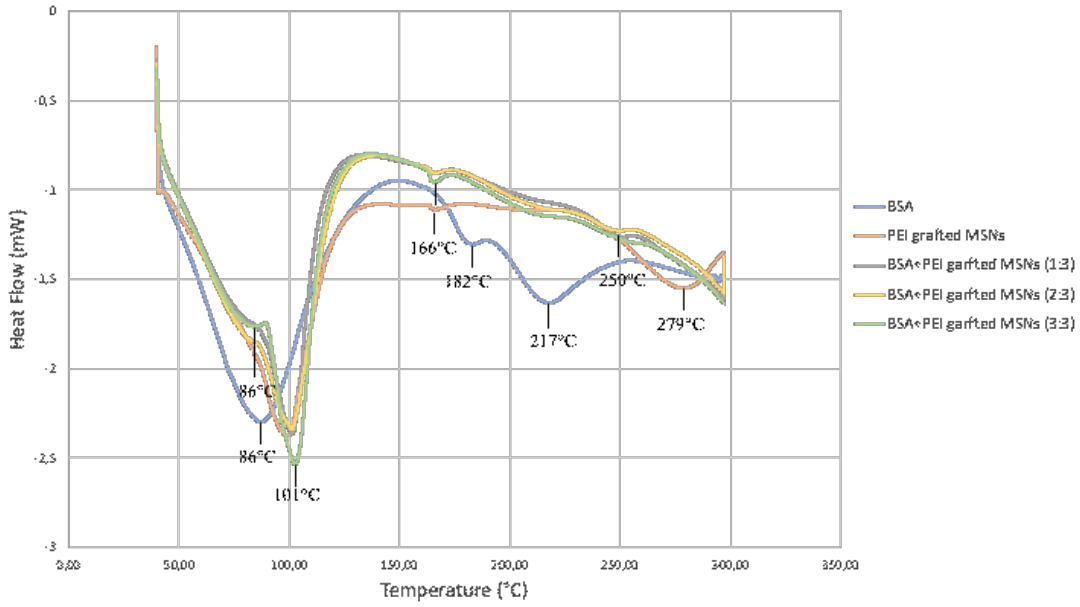

Figure 7 Differential scanning calorimetry (DSC) thermogram of BSA, PEI-grafted MSNs, and BSA-loaded PEI-grafted MSNs (1:3, 2:3, and 3:3 loading ratios of BSA to MSNs). Four main peaks are visible *at* 86 °C, 101 °C, 166 °C, *and* 182 °C

5.3 Surface plasmon resonance (SPR)

SPR interaction analysis was used to study the biofilm growth in real-time and the effects of ampicillin, PEI-grafted MSNs, and BSA-loaded PEI-grafted MSNs on the biofilm growth. Real-time SPR sensorgrams of *E. coli* biofilm formation and the effects of ampicillin (20 µg/ml, 100 µg/ml, and 300 µg/ml) with a no treatment as a control, are presented in **Figure 8**. The sensorgrams present the formation of a stable biofilm until the treatment. Addition of ampicillin resulted in a notable change in the thickness of the biofilm, while the control measurement presented no change.

Real-time SPR sensorgrams of the effects of MSNs, PEI-grafted MSNs and BSA-loaded PEI-grafted MSNs on *E. coli* biofilm formation are presented in **Figure 9**. Positively charged unloaded PEI-grafted MSNs resulted in a slightly decelerated biofilm growth. The other treatments did not result in notable changes in the biofilm formation.

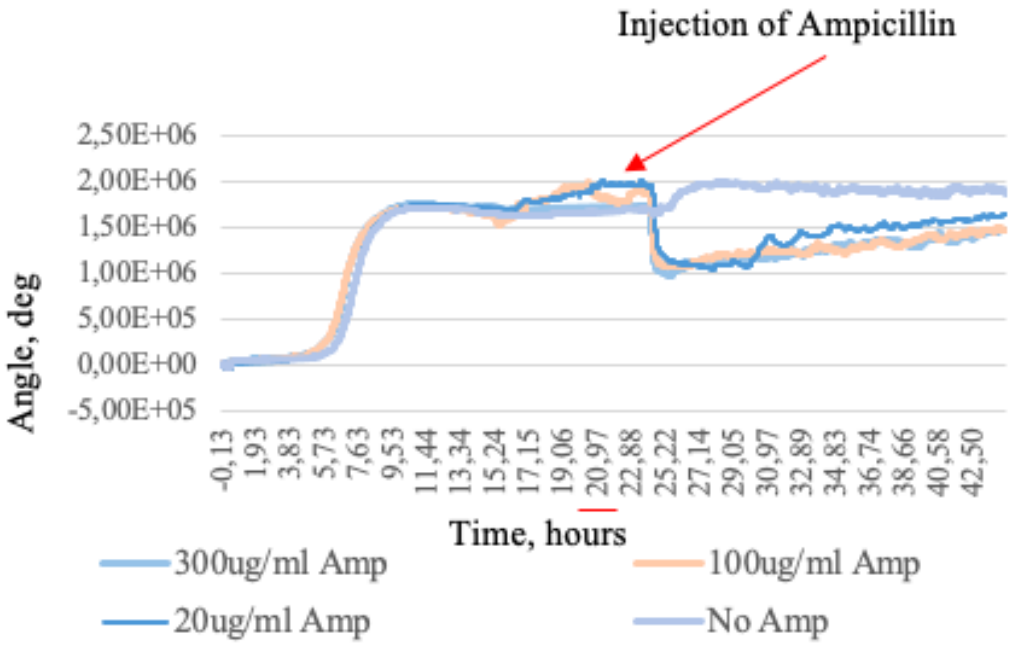

Figure 8 Surface plasmon resonance (SPR) sensorgrams of *E. coli* biofilm formation and the effects of ampicillin on the biofilm growth. *E. coli* biofilm was treated with ampicillin in Luria Broth (LB) with three concentrations (20 ug/ml, 100 ug/ml, and 300 ug/ml), with no treatment as a control. Ampicillin was added at a time point of 21 h, and the SPR measurement was continued with LB.

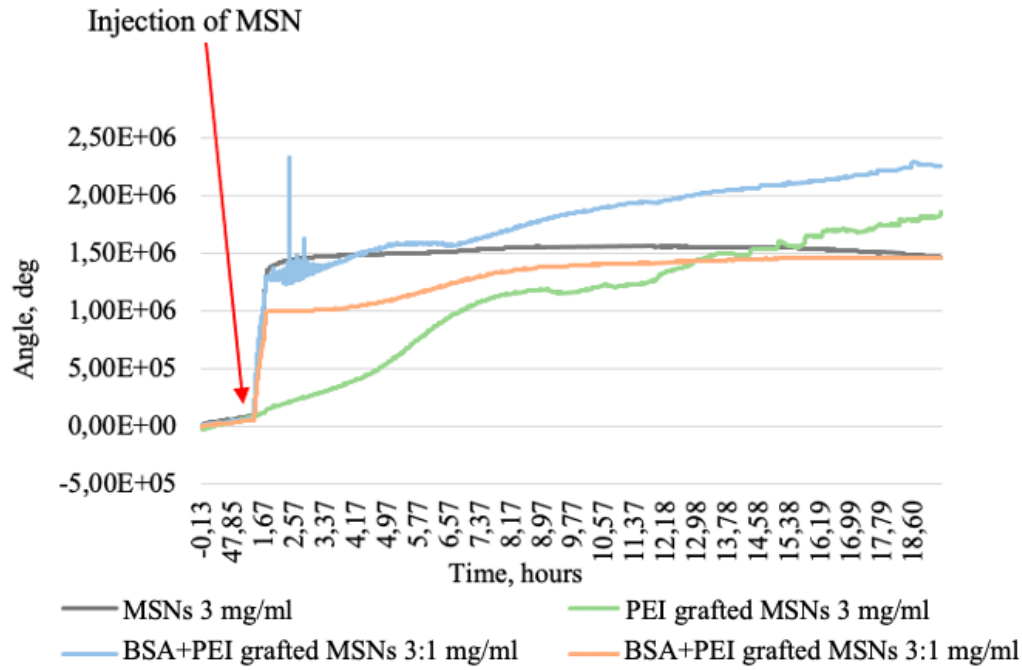

Figure 9 SPR sensorgrams of the effect of MSNs, PEI-grafted MSNs, and BSA-loaded PEI-grafted MSNs on *E. coli* biofilm formation. Samples of MSNs were injected to the biofilm at the beginning of the growth (ca. 1.5 h after bacteria injection) to visualize whether the biofilm formation was disrupted.

5.4 Confocal imaging

E. coli culture was visualized with confocal imaging after treatment of BSA and treatment of BSA-loaded PEI-grafted MSNs. In **Figure 11**, confocal images in green, red, and white light, and a composite image of *E. coli* culture treated for 48 hours with TRITC-labelled BSA-loaded PEI-grafted FITC-labelled MSNs. The composite image of confocal images taken in green, red, and white light presents the existence of BSA and MSNs throughout the biofilm. In the images, an aggregate of MSNs containing BSA is clearly notable.

Confocal images of *E. coli* culture treated with TRITC-labelled BSA for 48 hours are presented in **Figure 12** and **Figure 13**. In the composite images, the spread of BSA throughout the biofilm is visible. Some BSA aggregates are visible in both figures.

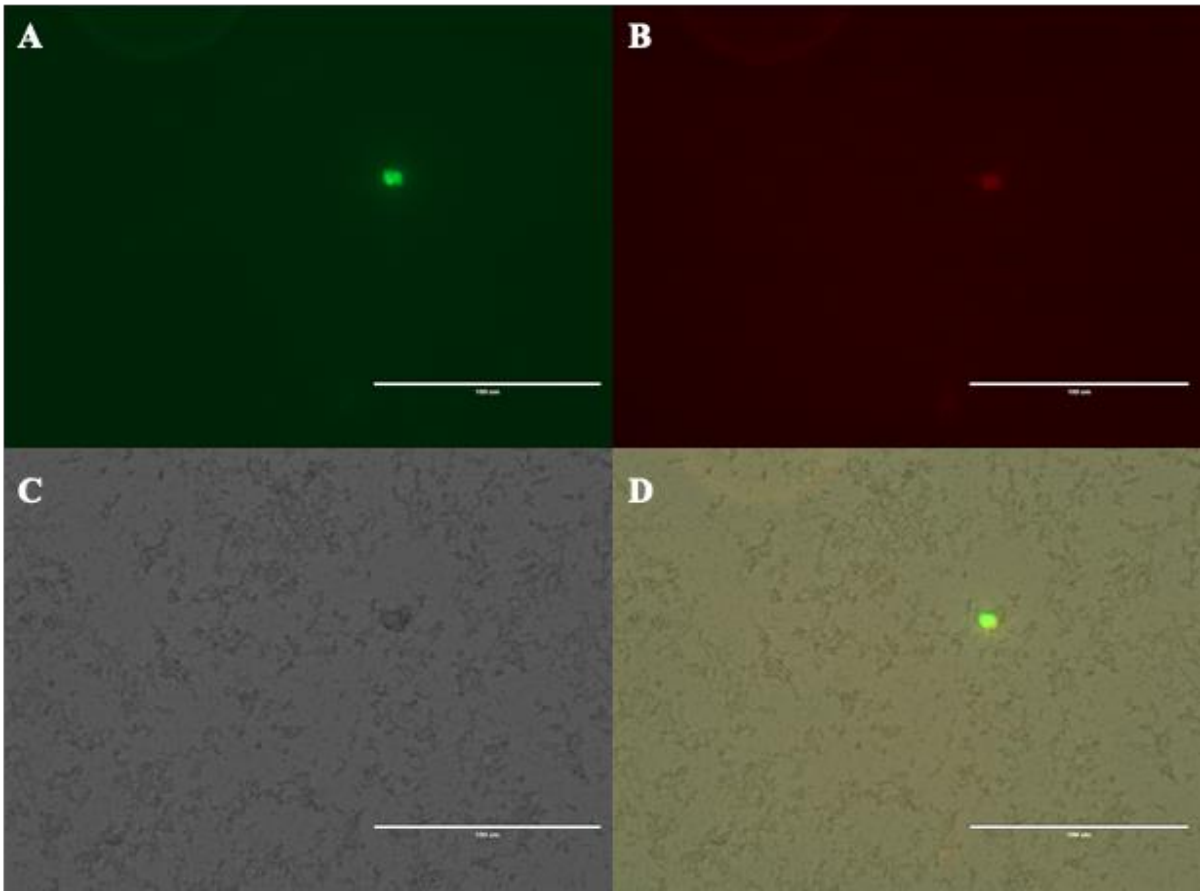

Figure 10 Confocal image of *E. coli* culture treated with BSA-loaded PEI-grafted MSNs for 48 hours in green, red, and white light. (A) FITC-labelled MSNs emit light at 519 nm resulting in a green glow, and (B) TRITC-labelled BSA emits light at 573 nm resulting in a red glow. Image taken with (C) white light visualizes the possible error sources and the non-fluorescent *E. coli* culture. (D) is a composite image of (A), (B), and (C) images. Scale bars, 100 µm.

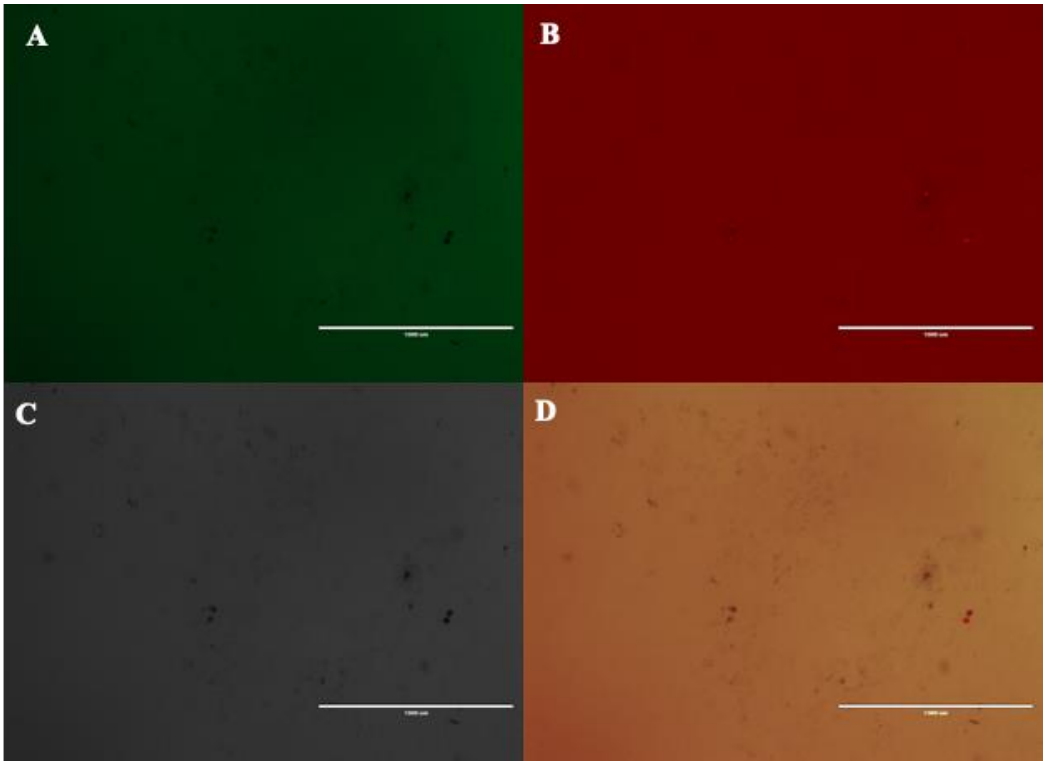

Figure 11 Confocal image of *E. coli* culture treated with fluorescent BSA for 48 hours in green (A), red (B) and white light (C). TRITC-labelled BSA emits light at 573 nm resulting in a red glow. Image (D) presents a composite of (A), (B) and (C). Scale bars, 1000 μm.

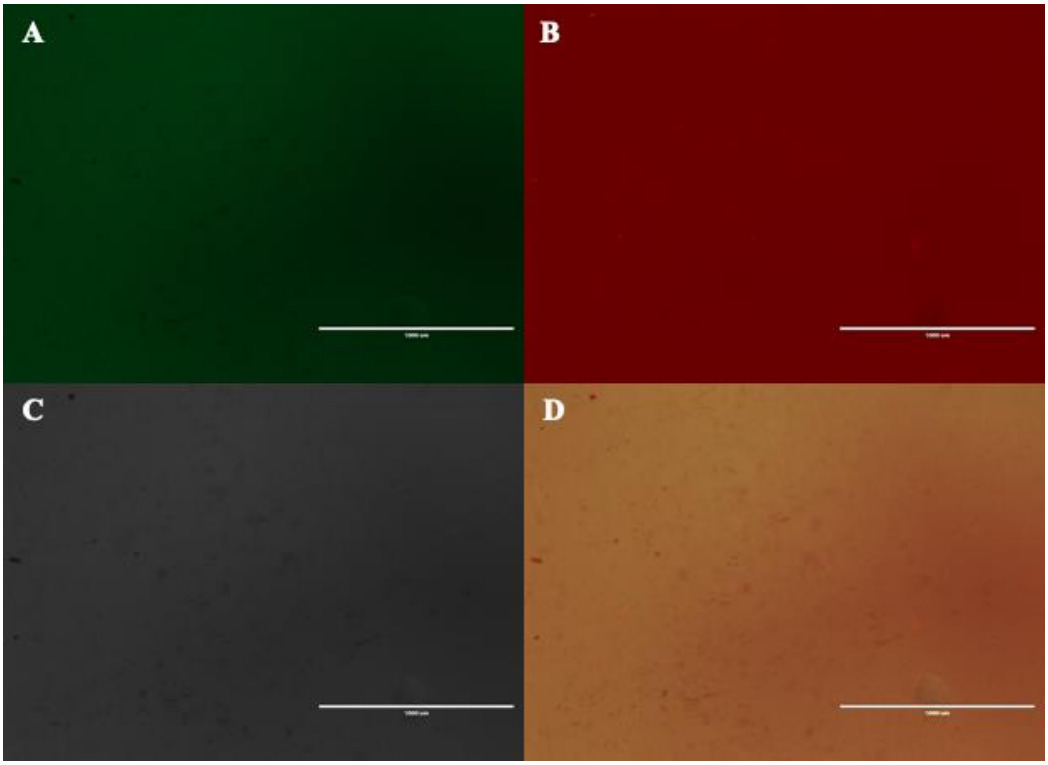

Figure 12 Confocal image of *E. coli* culture treated with fluorescent BSA for 48 hours in green (A), red (B) and white light (C). TRITC-labelled BSA emits light at 573 nm resulting in a red glow. Image (D) presents a composite of (A), (B) and (C). Scale bars, 1000 μm.

5.5 Short-term *in vitro* protein release

Short-term *in vitro* protein release was carried out in three different pHs representing the pH gradient within biofilms (pH 6, 6.5, and 7). The results plotted in a release graph with the percentage of BSA released from PEI-grafted MSN against time (min) are presented in **Figure 13**. The first measurement at timepoint 0 min presented a release of 60% to almost 100% of the protein cargo. In all pHs, the timepoint 0 presented the highest release, while the latter timepoints presented release between 40 to 90% of the protein cargo.

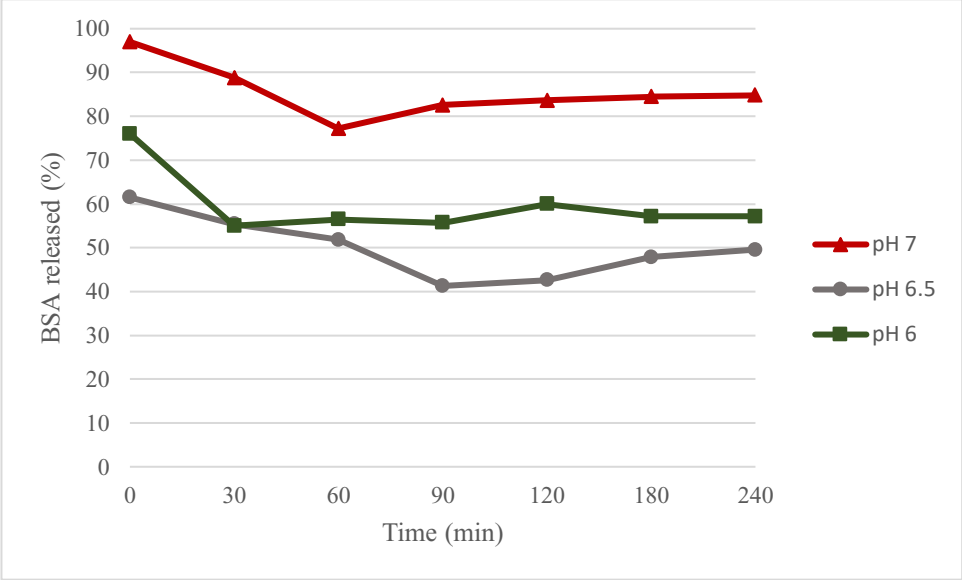

Figure 13 Short-term *in vitro* protein release curve. Short-term (4 hours) release of BSA from PEI-grafted MSNs presented as percentage of BSA released against time (min) in pH 6, 6.5, and 7. The chosen pH range represents the pH gradient within biofilms.

6 Discussion

During the past decades, MSNs as DDS have been widely explored to transport large amounts of therapeutic molecules to precise locations with enhanced efficacy and reduced side-effects (Manzano & Vallet-Regí, 2020). MSNs have been studied as a potential DDS for antimicrobial agents to biofilms, which are difficult to erase with traditional treatments (Xiu et al., 2021). In antibiofilm applications, the use of MSNs as drug carriers is aimed at overcoming biofilm-related resistance mechanisms and, thus, enhancing the therapeutic efficacy of antibiotics. In this study, MSNs were explored as potential nanocarriers for proteins for antibiofilm applications. BSA, a therapeutically inactive protein, was chosen as the placeholder protein for this study due to its similarity in size with a known protein, DegP, with suspected antibiofilm action (Fang et al., 2017). The MSN synthesis was performed according to the biphase stratification system protocol presented by Shen et al. (2014), yielding MSNs of uniform size and an adjusted pore size. The pore size of 10 nm was chosen for optimal protein loading and was achieved by adjusting the concentration of the used TEOS solution to 10%v/v in 99.5% cyclohexane.

According to the characterization studies, the used method yielded MSNs with a radial hydrodynamic size of 188 nm in average and radial size of 109 nm in diameter according to the MSNs visualized in TEM image. The hydrodynamic size is usually larger than size detected with TEM due to the differences in methods; DLS measurement is an intensity-based technique, and it puts higher emphasis on larger particles due to their stronger scattered light intensity, thus, any agglomeration can affect the results. Similarly, the TEM analysis only covers a limited sample, hence, it does not represent the variation of size accurately. Also, DLS measures the particle size in solution resulting in a hydration layer around the NPs, while TEM image is taken of dried form of the NPs. The hydrodynamic size of the MSNs with PEI grafting decreased to 177 nm. The decrease in size can be due to decrease in the hydration layer around the MSNs, as plain silica surface is highly hydrophilic and forms a very thick hydration layer, while PEI has some hydrophobic patches in the structure which decreases the thickness of the hydration layer.

The PdI value is a parameter that refers to the size range of the NPs. The term “polydispersity” describes the degree of non-uniformity of the size distribution. The value of PdI ranges from 0.0 to 1.0, with the latter indicating a highly polydisperse size distribution (Clarke, 2013).

In practice, PdI values of 0.2 and below are considered acceptable, and this limit was also chosen as the acceptable limit for this project. The synthesis method employed for this project yielded MSNs with PdI values within the acceptable size range. PEI grafting of the MSNs did not significantly change the PdI value, which indicates a successful homogenous coating of the particles. Fluorescent (FITC-conjugated) MSNs showed increased variation in the size range, however, as fluorescence is known to distort the measurement, the slightly increased size distribution was not expected to affect the results.

The ζ-potential value referring to the net surface charge of the NPs was measured for MSNs with and without PEI grafting. The silica surface is usually negatively charged due to various hydroxyl groups (Si-O-). The method employed in this study yielded MSNs with an average net surface charge of -18 mV. The non-covalent attachment of PEI generating a cationic surface yielded MSNs with a net surface charge of +28 mV, indicating that PEI grafting of the MSNs was successful. Positive net surface charge was desired to enable loading of the negatively charged protein by electrostatic interaction.

The characterization of the MSNs proved that the synthetized NPs were of adequate quality and could be further used for the following step, protein loading. The protein loading was done with the purpose to encapsulate an antibacterial protein, DegP, with a weight of 50.4 kDa (Fang et al., 2018). BSA was chosen as the model protein for loading due to its good availability, low price and, most importantly, similarity in size (66.5 kDa) with DegP (Uniprot, 2022). MES buffer with a pH of 4 was chosen as the loading medium due to conformational knowledge of BSA from literature. According to Penkov et al. (2017) in pH 3.5-4.5, BSA undergoes partial unfolding resulting in an F-form (fast) of the protein. This slightly more linear form was exploited to aid in the loading of the macromolecule into the pores of the MSNs. The isoelectric point (pI) of BSA is between pH 4.5 and 4.8 (Raghuwanshi et al. 2020). In the chosen pH for loading, BSA has slightly negative or positive (close to the pI of BSA) surface charge depending on the BSA concentration. Higher pHs would have ensured negative surface charge, however, the globular form of the protein in higher pHs might have complicated the encapsulation process. As no therapeutically active protein was used in this study, no attention was paid on whether the change in protein folding affects the activity of the protein. In further studies, it should be investigated whether the protein refolds back into the native and active structure after it has been released.

The loading protocol yielded an average LC% of 30%, with saturation taking place already in 1:3 ratio of BSA to MSNs. The accuracy of the concentration measurement in NanoDrop was deficient, as it could not provide the correct concentrations even for the control samples. This might have occurred due to poor blending of the protein suspension prior to the measurements.

The protein-loaded MSNs were freeze-dried for preservation, and the effect of freeze-drying was examined with ζ-potential measurements. The surface charge grew in each sample, even in the control, after freeze-drying. There was no obvious explanation for this change, however, a change might have occurred in PEI. It needs to be further examined if this change in the net surface charge affects the structural activity of the loaded protein. As for the therapeutic goal of MSN-encapsulated DegP-protein, it is necessary that the antibiofilm function would remain after treatments needed for the loading.

Characterization of the protein-loaded MSNs with DSC heat flow analysis suggests presence of BSA in the MSNs. BSA was characterized by an endothermic peak appearing at approximately 86 °C, suggesting denaturation of the protein at the temperature in question. A faint peak at this temperature was also found for samples of MSNs loaded with BSA, most visible for 3:3 ratio of BSA to MSNs, suggesting presence of BSA within the MSNs. PEI-grafted MSNs were characterized by an endothermic peak at approximately 100 °C. This peak was found in DSC curves of all samples containing PEI-grafted MSNs but was absent in the DSC curve of BSA. As all samples containing MSNs had been dissolved in a buffer prior to drying, a possible explanation for this peak is that some residues of the buffer dried and settled on the particles and burned at this point. The buffer residues could also explain the variations in the ζ-potential measurement of freeze-dried MSNs (Inam et al., 2022). As suggested previously, the loading of BSA to PEI-grafted MSNs reaches a saturation around 1:3 ratio of BSA to MSNs. This suggestion is enforced by the DSC scan as all the BSA-loaded MSNs samples show similar intensity in the observed peaks, indicating that they all contain similar amount of protein.

As part of this project, biofilm growth was monitored with real-time sensorgrams produced by the SPR technique. Real-time observation of biofilm growth with the SPR technique provides information about bacterial adhesion as well as a platform to visualize the effects of antibacterial agents on biofilms. The SPR technique has been previously used to study

bacterial adhesion to different materials as well as biofilm formation and removal (Pranzetti et al., 2012; Abadian et al., 2013). In this project, the antibiotic effect of ampicillin on *E. coli* biofilm was visualized with SPR sensorgrams where a decrease in the SPR angle correlates to decrease of the biofilm thickness. The SPR sensorgrams were used to visualize the growth of the *E. coli* biofilm and to compare the effect of different concentrations of ampicillin on biofilm thickness. All samples treated with different concentrations of ampicillin showed a notable decrease of the biofilm thickness in the sensorgrams, while the control measurement showed no change in biofilm thickness. The decrease in biofilm thickness is directly proportional to the number of bacteria living as part of the biofilm, thus, the decrease in thickness signifies a decrease in biofilm vitality.

To corroborate that MSNs have no intrinsic antimicrobial effect, SPR sensorgrams depicting the growth of different *E. coli* biofilms exposed to NP configurations were employed. Positively charged unloaded PEI-grafted MSNs resulted in a slightly decelerated biofilm growth. Most bacterial cells have a net negative surface charge (Wilson et al., 2001). The positive charge of unloaded PEI-grafted MSNs might have caused some electrostatic attraction between the MSNs and bacterial cells that could explain the slower biofilm growth. Other treatments did not result in notable changes in the biofilm formation, as the biofilm thickness grew undisturbed despite the addition of the MSNs and BSA-loaded PEI-grafted MSNs. Thus, the SPR analysis on biofilm growth produced expected results confirming that the antibiotic effect of ampicillin can be observed even at low concentrations and that MSNs by themselves have no antibiotic effect.

E. coli culture treated with BSA-loaded PEI-grafted MSNs was imaged using a confocal microscope to visualize the location of BSA and the NPs. The location of BSA does not completely overlap with the location of the MSNs, indicating that some amount of the protein has been released from the NPs. An agglomerate of MSNs containing BSA was visualized in the image. Agitation of the bacterial culture could be used in future studies to ensure equal distribution of the NPs. Consecutive images of different planes would be needed to achieve complete understanding of the location and potential interactions of the NPs throughout the bacterial culture. Additionally, a confocal image of an *E. coli* culture exposed solely to BSA was taken to visualize complete dispersion and release of the protein from the MSNs. Some protein agglomerations were observed, however, with the available

data, it cannot be conclusively proven that these agglomerates have been caused by interactions between the protein and bacteria.

The short-term *in vitro* protein release study performed in three different pHs corresponding to the pH gradient within *E. coli* biofilms resulted in an immediate release of more than 50% of the total protein amount in every studied pH. Interestingly, the amount of released protein decreased with time. As the pH used for loading the protein was noticeably lower, the significant change in pH might have caused the immediate release of BSA from the MSNs. Over time, the released BSA might have re-interacted with the MSNs and reached an equilibrium, which could explain the protein release curve. To prevent immediate release of the protein cargo, the MSN-protein complex should be further modified to achieve controlled release. Premature release of the cargo is a common challenge, which has been addressed with a variety of gatekeeper elements, such as organic molecules, supramolecular assemblies, NPs, and microfluidic polymer coatings (Huang et al., 2020; Kücüktürkmen et al., 2022). In future experiments, a gatekeeper element could be added to the currently studied MSN-protein complex to achieve more favorable results.

7 Conclusions

MSNs could be used as drug delivery vehicles for antibiofilm applications to obtain more precise delivery of antibiotics and enhanced therapeutic efficacy. Biofilms display several resistance mechanisms that could be overcome with MSNs. In this project, MSNs were explored as a potential carrier system for DegP protein with suspected anti-biofilm action. The used MSN synthesis method yielded uniform size monodispersed NPs with the desirable dendritic porous structure. An average loading capacity of 30% was reached with the loading protocol for BSA used during this study. Characterization of the protein-loaded MSNs conducted by DSC analysis demonstrated the characteristic thermal changes for the MSN-protein complex.

The SPR studies showed that MSNs have no intrinsic antimicrobial effect. Short-term *in vitro* protein release studies conducted in pHs corresponding to the pH gradient within biofilms unveiled premature release of protein cargo. This undesirable leakage should be

acted on by modifying the MSN-protein complex by adding e.g., a gatekeeper to achieve controlled release.

As demonstrated in this project, MSNs have potential to carry therapeutic proteins within their pores. The use of MSNs provides a wide range of possible design variations with controlled release, specific delivery, and protective shield for macromolecules. Further research is needed to examine the complete potential of MSNs as drug delivery vehicles. This study has set out the baseline for how to load proteins of a size range similar to BSA into MSNs and how to study the antimicrobial effects of MSN-protein complexes.

8 Summary in Swedish – Svensk sammanfattning

Mesoporösa kiselnanopartiklar som proteinbärare för antibiofilmapplikationer

Multiresistenta bakterier orsakar ett växande globalt problem och är ett stort hot mot folkhälsan. Cirka 700 000 patienter dör av multiresistenta bakterier globalt varje år, och man har uppskattat att år 2050 kommer multiresistenta bakterier att orsaka över 10 miljoner dödsfall årligen. Cirka 60 till 70 % av bakterieinfektionerna är förknippade med bildning av biofilmer som är orsak till en mängd olika kroniska infektioner. Biofilmer är den naturliga livsstilen för mikroorganismer. Bakteriebiofilmer skyddar bakterier effektivt med flera mekanismer som hjälper till att hantera miljöstress och låter mikrober i biofilmer uppvisa en antibiotikaresistens som är upp till 1000 gånger högre än sina planktoniska motsvarigheter. Dessutom påskyndar biofilmer spridningen av resistensgener genom att erbjuda en gynnsam miljö för horisontell överföring av genetiskt material. För närvarande finns det bara ett fåtal effektiva antibiotika kvar för att behandla infektioner som orsakas av multiresistenta bakterier, och deras effektivitet minskar avsevärt när dessa bakterier bildar biofilmer.

För att bekämpa multiresistenta bakterier behövs nya tillvägagångssätt inom antibiotikaforskning. För närvarande finns det inga läkemedelsprodukter som skulle ha godkänts för att specifikt behandla biofilmrelaterade infektioner. En av huvudutmaningarna

är leveransen av antibiotika till bakteriella biofilmer så att terapeutiska koncentrationer av läkemedlet uppnås. Nanomedicin tillhandahåller nya verktyg för att bekämpa detta problem; läkemedelsbärare i nanostorlek har undersökts som system för tillförsel av läkemedel för leverans av antimikrobiella medel till biofilmer. Fördelarna med system för läkemedelstillförsel i nanostorlekar inkluderar förbättrad penetration och ackumulering av antibiotika i biofilmer, vilket ger ökad effektivitet och minskade biverkningar. Forskningen av nya system för läkemedelstillförsel måste utvecklas tillsammans med nya antimikrobiella terapier för att övervinna problemet med multiresistenta bakterier. I detta projekt utforskades mesoporösa kiselnanopartiklar (MSN) som ett potentiellt bärarsystem för DegP-protein med misstänkt antibiofilmverkan. Mesoporösa kiselnanopartiklar valdes på grund av deras anpassningsbarhet, låga pris och förväntade biokompatibilitet. Användningen av terapeutiskt aktiva proteiner föll inte inom ramen för denna studie; därför användes ett platshållarprotein, bovint serumalbumin (BSA), för att definiera proteinladdningsprotokollet och analys av de laddade mesoporösa kiselnanopartiklar.

MSN-syntesen utfördes enligt protokollet för tvåfasstratifierinssystem. Porstorleken justerades till 10 nm genom att kontrollera de hydrofoba lösningsmedlen och koncentrationen av kiseldioxinkällan i den övre oljefasen. Både optiskt transparenta och fluorescerande MSN utfördes. Alla syntetiserade MSN modifierades med ympning av polyetylenimin (PEI) för att ändra ytladdningen från negativ till positiv för att optimera proteinladdningen. Den hydrodynamiska partikelstorleken (⌀ nm) och ytladdningen bekräftades med analys av dynamisk ljusspridning (DLS). En transmittanselektronmikroskopi (TEM) bild togs för att visualisera och bekräfta storleken på och enhetligheten hos MSN. Resultaten visade att den använda MSN-syntesmetoden gav monodispergerade nanopartiklar med en enhetlig storlek på den önskvärda dendritiska porösa strukturen. Enligt DLS-analysen var nanopartiklarna av en storlek kring 188 nm.

Proteinladdningen utfördes för tre olika koncentrationer (1 mg/ml, 2 mg/ml och 3 mg/ml) av BSA till 3 mg av PEI-ympade MSN med MES-buffert (pH 4) som laddningsmedium. Laddningen utfördes genom att sonikera proverna under 30 sekunder. Proverna centrifugerades vid 12 300 x g i 20 minuter två gånger och belastningskapaciteten (LC%) beräknades med avseende på den totala mängden protein som uppmätts i supernatanter som samlats under lastningen. En genomsnittlig LC% på 30 % uppnåddes med det använda laddningsprotokollet för BSA som utvecklats under denna studie. Karakterisering av de

proteinladdade mesoporösa kiselnanopartiklarna utfördes med analys av differentiell svepkalorimetri (DSC). Resultaten visade närvaro av modellproteinet i nanopartiklarna.

Analys av ytplasmonresonans (SPR) användes för att studera biofilmtillväxten i realtid och och effekterna av MSN och MSN-proteinkomplexet på biofilmtillväxten. I den första SPR-analysen behandlades den bildade *E. coli*-biofilmen med 20 ug/ml, 100 ug/ml och 300 ug/ml ampicillin med ingen behandling som kontroll. I den andra analysen behandlades *E. coli*-biofilmen med MSN, PEI-ympade MSN och BSA-laddade PEI-ympade MSN. SPR-studierna visade att mesoporösa kiselnanopartiklar inte har någon inneboende antimikrobiell effekt. För att visualisera närvaron av BSA och MSN i *E. coli*-kultur togs konfokala bilder.

Kortvariga in vitro-studier av proteinfrisättning i fosfatbuffrad saltlösning (PBS) utfördes för tre olika pH-värden (6, 6,5 och 7) som representerar den naturliga pH-gradienten i *E. coli*-biofilmer. För varje pH placerades triplikat av sju tidpunkter (0 min, 30 min, 60 min, 90 min, 120 min, 180 min och 240 min) med 0,5 mg/ml BSA-laddade PEI-ympade MSN i ett skakande vattenbad vid 37°C och absorbansen mättes vid 285 nm vid motsvarande tidpunkter. Resultaten avslöjade för tidig frisättning av proteinlasten. Detta oönskade läckage bör åtgärdas genom att modifiera mesoporösa kiselnanopartikel-proteinkomplexet genom att lägga till t.ex. en ’’gatekeeper’’ för att uppnå kontrollerad frisättning.

Som visats i detta projekt har mesoporösa kiselnanopartiklar potential att bära terapeutiska proteiner i sina porer. Andvändningen av mesoporösa kiselnanopartiklar get ett brett utbud av möjliga desingvariationer med kontrollerad frisättning, specifik leverans och skyddande sköld för makromolekyler. Ytterligare forskning behövs för att undersöka den fullständiga potentialen hos mesoporösa kiselnanopartiklar som läkemedelsleveransbärare. Denna studie har angett grund på för hur man laddar proteiner i ett storleksintervall som liknar BSA till mesoporösa kiselnanopartiklar och hur man studerar de antimikrobiella effekterna av nanopartikel-proteinkomplex.

9 References

A.-K. John, M. Schmaler, N. Khanna and R. Landmann, Antimicrob. Agents Chemother., 55 (3510–3516), 2011

Abadian, P.N., Tandogan, N., Jamieson, J.J., Goluch, E.D.: Using surface plasmon resonance imaging to study bacterial biofilms. Biomicrofluidics. 8, 2014

Angles, M.L., Marshall, K.C., Goodman, A.E.: Plasmid transfer between marine bacteria in the aqueous phase and biofilms in reactor microsoms. Appl. Environ. Microbiol. Vol. 59 (843-859), 1993

Beloin, C., Renard, S., Ghigo, J.-M., Lebeaux, D.: Novel approaches to combat bacterial biofilms. Current Opinion in Pharmacology. Vol. 18 (61-68), 2014

Bhutani, P., Joshi, G., Raja, N., Bachhav, N., Rajanna, P.K., Bhutani, H., Paul, A.T., Kumar, R.: U.D. FDA Approved Drugs from 2015 – June 2020: A Perspective. Journal of Medicinal Chemistry. Vol. 64 (2339-2381), 2021

Bindini, E., Chehabi, Z., Faustini, M., Albouy, P.-A., Grosso, D., Gattoni, A., Chanéac, C., Azzaroni, O., Sanchez, C., Boissière, C.; Following in Situ the Degradation of Mesoporous Silica in Biorelevant Conditions: At Last, a Good Comprehension of the Structure Influence. Applied Materials & Interfaces. 12 (13598-13612), 2020

Blanco, P., Hernando-Amado, A., Reales-Calderon, J.A., Corona, F., Lira, F., Alcalde-Rico, M., Bernardini, A., Blanca Sanchez, M., Martinez, J.L.: Bacterial Multidrug Efflux Pumps: Much More Than Antibiotic Resistance Determinants. Microorganisms. Vol. 4:14, 2016,

Ceri, H., Olson, M.E., Stremick, C., Read, R.R., Morck, D., Buret, A.: The Calgary Biofilm Device: New Technology for Rapid Determination of Antibiotic Susceptibilities of Bacterial Biofilms. Vol. 37 (No. 6), 1999

Clarke, S. Development of Hierarchical Magnetic Nanocomposite Materials for Biomedical Applications. Ph.D. Thesis, Dublin City University, Northside, Dublin, 2013

Cui, Y., Dong, H., Cai, X., Wang, D., and Li, Y.; Mesoporous silica nanoparticles capped with disulfide-linked PEG gatekeepers for glutathione-mediated controlled release. *ACS Appl. Mater. Interfaces* 4, 3177–3183, 2012

D'souza, A. A., and Shegokar, R.; Polyethylene glycol (PEG): a versatile polymer for pharmaceutical applications. *Expert Opin. Drugs Deliv*. 13, 1257–75, 2016

Davies, D. G., M. R. Parsek, J. P. Pearson, B. H. Iglewski, J. W. Costerton, and E. P. Greenberg. The involvement of cell-to-cell signals in the development of a bacterial biofilm. Science. 280 (295–298), 1998

Deodhar, G., Adams, M.L., Trewyn, B.G.: Controlled release and intracellular protein delivery from mesoporous silica nanoparticles. Biotechnology Journal. Vol. 12, 2017

Diab, R., Canilho, N., Pavel, I.A., Haffner, F.B., Girardon, M., Pasc, A.; Silica-Based systems for oral delivery of drugs, macromolecules and cells. Advances in Colloid and Interface Science. 249 (346-362), 2017

Dong Y, Zhang L. Quorum sensing and quorum-quenching enzymes. J Microbiol. Vol. 43 (101-9), 2005

Fang, Kuili, Xing Jin, and Seok Hoon Hong.; Probiotic Escherichia Coli Inhibits Biofilm Formation of Pathogenic E. Coli via Extracellular Activity of DegP. Scientific Reports 8 (1): (1–12), 2018

Flemming H-C, Wingender J, Griegbe, Mayer C. Physico-chemical properties of biofilms. In: Evans LV, editor. Biofilms: recent advances in their study and control. Amsterdam: Harwood Academic Publishers. p. 19–34, 2012

Flemming, H.-C., Wingender, J., Szewzyk, U., Steinberg, P., Rice, S.A., Kjelleberg, S.: Biofilms: an emergent form of bacterial life. Nature Reviews Microbiology. Vol. 14 (563-576), 2016

Food and Drug Administration (FDA). GRAS Notices. [Available at: https://www.cfsanappsexternal.fda.gov/scripts/fdcc/?set=GRASNotices&sort=GRN_No&order=DESC&startrow=1&type=basic&search=sili], 2022

Fulaz, S., Hiebner, D., Barros, C.H.N., Devlin, H., Vitale, S., Quinn, L., Casey, E.; Radiometric Imaging of the in Situ pH Distribution of Biofilms by Use of Fluorescent Mesoporous Silica Nanosensors. Applied Materials & Interfaces. 11 (32769-32688), 2019

Fuqua, C., Greenberg, E.P.; Cell-to-cell communication in Escherichia coli and Salmonella typhimurium: They may be talking, but who's listening? The Proceedings of the National Academy of Sciences (PNAS). Vol. 95 (6571-6572), 1998

Garrett, E. S., D. Perlegas, and D. J. Wozniak.; Negative control of flagellum synthesis in Pseudomonas aeruginosa is modulated by the alternative sigma factor AlgT (AlgU). Journal of Bacteriology. 181:7401–7404, 1999

Hall-Stoodley, L., Stoodley, P.; Evolving concepts in biofilm infections. Cellular Microbiology. Vol. 11:7 (1034-1043), 2009

Hausner M, Wuertz S.; High rates of conjugation in bacterial biofilms as determined by quantitative in situ analysis. Appl Environ Microbiol. 65:3710–13, 1999

Hausner, M., Wuertz, S.; High rates of conjugation in bacterial biofilms as determined by quantitative in situ analysis. Appl. Environ. Microbiol. Vol. 65 (3710-3713), 1999

Hidalgo, G., Burns, A., Herz, E., Hay, A.G., Houston, P.L., Wiesner, U., Lion, L.W.; Functional tomographic fluorescence imaging of pH microenvironments in microbial biofilms by use of silica nanoparticle sensors. Applied and Environmental Microbiology. 75 (23): 2426-7435, 2009

Hoiby, N.; A short history of microbial biofilms and biofilm infections. Acta Pathologica, Microbiologica et Immunologica Scandinavica (APMIS). 125 (272-275), 2017

Hook, A., Chang, CY., Yang, J.; Combinatorial discovery of polymers resistant to bacterial attachment. *Nat Biotechnol* 30, 868–875, 2012

Huang, R., Shen, Y.-W., Guan, Y.-Y., Jiang, Y.-X., Wu, Y., Rahman, K., Zhang, L.-J., Liu, H.-J., Luan, X.; Mesoporous silica nanoparticles: facile surface functionalization and versatile biomedical applications in oncology. Acta Biomaterialia. Vol. 116:1-15, 2020

Iler, R.K.; The Chemistry of Silica: Solubility, Polymerization, Colloid and Surface Properties, and Biochemistry of Silica. John Wiley and Sons Ltd., New York. 1979

Inam, W., Bhadane, R., Akpolat, R.N., Taiseer, R.A., Filippov, S.K., Salo-Ahen, O.M.H., Rosenholm, J.M., Zhang, H.; Interactions between polymeric nanoparticles and different buffers as investigated by zeta potential measurements and molecular dynamics simulations. View. 2022

Jokerst, J. V., Lobovkina, T., Zare, R. N., and Gambhir, S. S.; Nanoparticle PEGylation for imaging and therapy. *Nanomedicine* 6, 715–728, 2011

Kücüktürkmen, B., Inam, W., Howaili, F., Gouda, M., Prabhakar, N., Zhang, H., Rosenholm, J.M.; Microfluidic-Assisted Fabrication of Dual-Coated pH-Sensitive Mesoporous Silica Nanoparticles for Protein Delivery. Biosensors. 12 (181), 2022

Leclerc, L., Rima, W., Boudard, D., Pourchez, J., Forest, V., Bin, V.; Size of submicrometric and nanometric particles affect cellular uptake and biological activity of macrophages *in vitro*. *Inhal. Toxicol.* 24 (580–588), 2012

Lewandowski Z.; Structure and function of biofilms. In: Evans LV, editor. Biofilms: recent advances in their study and control. Amsterdam: Harwood Academic Publishers; p. 1–17, 2000

Liu, H.-J., Xu, P.; Smart Mesoporous Silica Nanoparticles for Protein Delivery. Nanomaterials. Vol. 9 (511), 2019

Mah, T. F., O'Toole, G. A.; Mechanisms of biofilm resistance to antimicrobial agents. Trends in Microbiology. Vol. 9 (34–39), 2001

Manzano, M., Vallet-Regí, M.; Mesoporous Silica Nanoparticles for Drug Delivery. Advanced Functional Materials. (30), 2020

McLean, R. J., Whiteley M., Strickler D. J., Fuqua W. C.; Evidence of autoinducer activity in naturally occurring biofilms. FEMS Microbiol. Lett. 154:259–263, 1997

Milo, R., Phillips, R.; Cell Biology by the numbers. Garland Science, Taylor and Francis Group. 2015

Min, Y., Caster, J.M., Eblan, M.J., Wang, A.Z.; Clinical Translation of Nanomedicine. American Chemical Society. 115 (11147-11190), 2015

Muhammad, M.H., Idris, A.L., Fan, X., Guo, Y., Yu, Y., Jin, X., Qiu, J., Guan, X., Huang, T.; Beyond Risk: Bacterial Biofilms and Their Regulating Approaches. Frontiers in Microbiology. Vol. 11, 2020

Penkov, N., Yashin, V., Fesenko Jr, E., Manokhin, A., Fesenko, E.; A Study of the Effect of a Protein on the Structure of Water in Solution Using Terahertz Time-Domain Spectroscopy. Applied Spectroscopy. 2017

Pranzetti, A., Salaün, S., Mieszkin, S., Callow, M.E., Callow, J.A., Preece, J.A., Mendes, P.M.; Model Organic Surfaces to Probe Marine Bacterial Adhesion Kinetics by Surface Plasmon Resonance. Advanced Functional Materials. Vol. 22 (17), 2012

Prigent-Combaret, C., Vidal O., Dorel C., Lejeune P.; Abiotic surface sensing and biofilm-dependent regulation of gene expression in Escherichia coli. Journal of Bacteriology. 181 (5993–6002), 1999

Raghuwanshi, V.S., Yu, B., Browne, C., Garnier, G.; Reversible pH Responsive Bovine Serum Albumin Sponge Nanolayer. Frontiers in Bioengineering and Biotechnology. 2020

Rosenholm, J.M., Penninkangas, A., Lindén, M.; Amino-functionalization of large-pore mesoscopically ordered silica by a one-step hyperbranching polymerization of a surface-grown polyethyleneimine. The Royal Society of Chemistry. (3909-3911), 2006

Schaenzer, A.J., Wright, G.; Antibiotic Resistance by Enzymatic Modification of Antibiotic Targets. Trends in Molecular Medicine. Vol. 25:8, 2020

Schlafer, S., Baelum, V., Dige, I.; Improved pH-ratiometry for the three-dimensional mapping of pG microenvironments in biofilms under flow conditions. Journal of Microbiological Methods. Vol. 152 (194-200), 2018

Selvarajan, V., Obuobi, S., Ee, P.L.R.; Silica Nanoparticles - A Versatile Tool for the Treatment of Bacterial Infections. Frontiers in Chemistry. Vol. 8, 2020

Shen, D., Jianping, Y., Xiaomin, L., Lei, Z., Renyuan, Z., Wei, L., Lei, C., Rui, W., Fan, Z., Dongyuan, Z.; "Biphase Stratification Approach to Three-Dimensional Dendritic Biodegradable Mesoporous Silica Nanospheres." Nano Letters 14 (2): (923–32), 2014

Song, X., Liu, P., Liu, X., Wang, Y., Wei, H., Zhang, J., Yu, L., Yan, X., He, Z.; Dealing with MDR bacteria and biofilm in the post-antibiotic era: Application of antimicrobial peptides-based nano-formulation. Materials Science and Engineering. Vol. 128, 2021

Sweeney J.B.; Aziridines: epoxides' ugly cousins? The Royal Society of Chemistry. 31:247-258, 2002

Tang, F., Li, L., Chen, D.; Mesoporous Silica Nanoparticles: Synthesis, Biocompatibility and Drug Delivery. Advanced Materials. 24 (1504-1534), 2012

Tochilin, V.P.; Multifunctional nanocarriers. Advanced Drug Delivery Reviews. Vol. 64 (302-315), 2012

Uniprot; Bos taurus Albumin. [Available at: https://www.uniprot.org/uniprot/P02769], Accessed 10.3.2022

Wang, F., Zhang, L., Bai, X., Cao, X., Jiao, X., Huang, Y., Li, Y., Qin, Y., Wen, Y.: Stimuli-Responsive Nanocarrier for Co-delivery of MiR-31 and Doxorubicin to Suppress High MtEF4 Cancer. Applied Materials and Interfaces. Vol. 10 (22767-22775), 2018

Waters C, Bassler B.; Quorum sensing cell-to-cell communication in bacteria. Ann Rev Cell Dev Biol. 21, 2005

Watnick, P. I., Kolter R.; Steps in the development of a Vibrio cholerae biofilm. Mol. Microbiol. 34:586–595, 1999

Watnick, P., Kolter, R.; Biofilm, City of Microbes. Journal of Bacteriology. 2000, Vol. 182
Xiu, W., Shan, J., Yang, K., Xiao, H., Yuwen, L., Wang, L.: Recent development of nanomedicine for the treatment of bacterial infections. VIEW. (2), 2021

Wilson, W.W., Wade, M.M, Holman, S.C.; Champlin, F.R.; Status of methods for assessing bacterial cell surface charge properties based on zeta potential measurements. Journal of Microbiological Methods. 43 (3:153-164), 2001

Zhao, Y., Sun, X., Zhang, G., Trewyn, B. G., Slowing, I. I., and Lin, V. S.-Y.; Interaction of mesoporous silica nanoparticles with human red blood cell membranes: size and surface effects. *ACS Nano* 5, 1366–1375, 2011